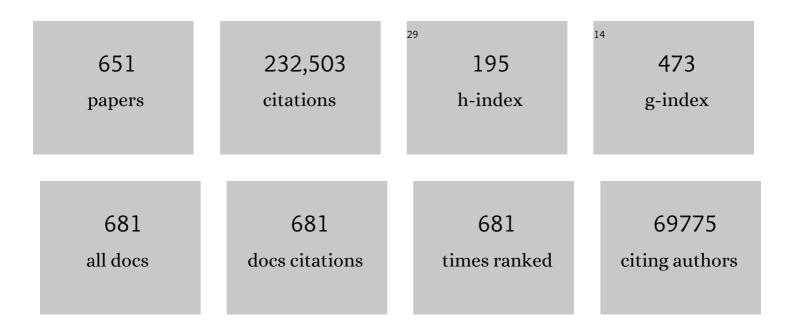
## Michael Grätzel

List of Publications by Year in descending order

Source: https://exaly.com/author-pdf/2426957/publications.pdf Version: 2024-02-01



#	Article	IF	CITATIONS
1	A low-cost, high-efficiency solar cell based on dye-sensitized colloidal TiO2 films. Nature, 1991, 353, 737-740.	13.7	26,665
2	Photoelectrochemical cells. Nature, 2001, 414, 338-344.	13.7	11,931
3	Sequential deposition as a route to high-performance perovskite-sensitized solar cells. Nature, 2013, 499, 316-319.	13.7	8,542
4	Lead Iodide Perovskite Sensitized All-Solid-State Submicron Thin Film Mesoscopic Solar Cell with Efficiency Exceeding 9%. Scientific Reports, 2012, 2, 591.	1.6	6,763
5	Long-Range Balanced Electron- and Hole-Transport Lengths in Organic-Inorganic CH <sub>3</sub> NH <sub>3</sub> Pbl <sub>3</sub> . Science, 2013, 342, 344-347.	6.0	6,060
6	Porphyrin-Sensitized Solar Cells with Cobalt (II/III)–Based Redox Electrolyte Exceed 12 Percent Efficiency. Science, 2011, 334, 629-634.	6.0	5,637
7	Cesium-containing triple cation perovskite solar cells: improved stability, reproducibility and high efficiency. Energy and Environmental Science, 2016, 9, 1989-1997.	15.6	4,560
8	Dye-sensitized solar cells with 13% efficiency achieved through the molecular engineering of porphyrin sensitizers. Nature Chemistry, 2014, 6, 242-247.	6.6	3,982
9	Solid-state dye-sensitized mesoporous TiO2 solar cells with high photon-to-electron conversion efficiencies. Nature, 1998, 395, 583-585.	13.7	3,353
10	Incorporation of rubidium cations into perovskite solar cells improves photovoltaic performance. Science, 2016, 354, 206-209.	6.0	3,137
11	Low-temperature solution-processed wavelength-tunable perovskites for lasing. Nature Materials, 2014, 13, 476-480.	13.3	2,725
12	A hole-conductor–free, fully printable mesoscopic perovskite solar cell with high stability. Science, 2014, 345, 295-298.	6.0	2,685
13	Molecular Photovoltaics. Accounts of Chemical Research, 2000, 33, 269-277.	7.6	2,625
14	Recent Advances in Sensitized Mesoscopic Solar Cells. Accounts of Chemical Research, 2009, 42, 1788-1798.	7.6	2,502
15	Engineering of Efficient Panchromatic Sensitizers for Nanocrystalline TiO2-Based Solar Cells. Journal of the American Chemical Society, 2001, 123, 1613-1624.	6.6	2,483
16	Efficient inorganic–organic hybrid heterojunction solar cells containing perovskite compound and polymeric hole conductors. Nature Photonics, 2013, 7, 486-491.	15.6	2,423
17	Water photolysis at 12.3% efficiency via perovskite photovoltaics and Earth-abundant catalysts. Science, 2014, 345, 1593-1596.	6.0	2,260
18	Synthesis and crystal chemistry of the hybrid perovskite (CH3NH3)PbI3 for solid-state sensitised solar cell applications. Journal of Materials Chemistry A, 2013, 1, 5628.	5.2	2,254

Michael Grã

#	Article	IF	CITATIONS
19	Pseudo-halide anion engineering for α-FAPbI3 perovskite solar cells. Nature, 2021, 592, 381-385.	13.7	2,095
20	Efficient and stable large-area perovskite solar cells with inorganic charge extraction layers. Science, 2015, 350, 944-948.	6.0	2,007
21	Highly active oxide photocathode for photoelectrochemical water reduction. Nature Materials, 2011, 10, 456-461.	13.3	1,894
22	The light and shade of perovskite solar cells. Nature Materials, 2014, 13, 838-842.	13.3	1,877
23	Mesoscopic CH <sub>3</sub> NH <sub>3</sub> Pbl <sub>3</sub> /TiO <sub>2</sub> Heterojunction Solar Cells. Journal of the American Chemical Society, 2012, 134, 17396-17399.	6.6	1,801
24	Polymer-templated nucleation and crystal growth of perovskite films for solar cells with efficiency greater thanA21%. Nature Energy, 2016, 1, .	19.8	1,719
25	Fabrication of thin film dye sensitized solar cells with solar to electric power conversion efficiency over 10%. Thin Solid Films, 2008, 516, 4613-4619.	0.8	1,702
26	Efficient luminescent solar cells based on tailored mixed-cation perovskites. Science Advances, 2016, 2, e1501170.	4.7	1,669
27	A vacuum flash–assisted solution process for high-efficiency large-area perovskite solar cells. Science, 2016, 353, 58-62.	6.0	1,636
28	Growth of CH3NH3PbI3 cuboids with controlled size for high-efficiency perovskite solar cells. Nature Nanotechnology, 2014, 9, 927-932.	15.6	1,600
29	Promises and challenges of perovskite solar cells. Science, 2017, 358, 739-744.	6.0	1,510
30	New Benchmark for Water Photooxidation by Nanostructured α-Fe2O3Films. Journal of the American Chemical Society, 2006, 128, 15714-15721.	6.6	1,477
31	A stable quasi-solid-state dye-sensitized solar cell with an amphiphilic ruthenium sensitizer and polymer gel electrolyte. Nature Materials, 2003, 2, 402-407.	13.3	1,466
32	Nanocrystalline Titanium Oxide Electrodes for Photovoltaic Applications. Journal of the American Ceramic Society, 1997, 80, 3157-3171.	1.9	1,418
33	Perovskite solar cells employing organic charge-transport layers. Nature Photonics, 2014, 8, 128-132.	15.6	1,320
34	Electrochemical and Photoelectrochemical Investigation of Single-Crystal Anatase. Journal of the American Chemical Society, 1996, 118, 6716-6723.	6.6	1,312
35	Enhance the Optical Absorptivity of Nanocrystalline TiO <sub>2</sub> Film with High Molar Extinction Coefficient Ruthenium Sensitizers for High Performance Dye-Sensitized Solar Cells. Journal of the American Chemical Society, 2008, 130, 10720-10728.	6.6	1,307
36	Perovskite solar cells with CuSCN hole extraction layers yield stabilized efficiencies greater than 20%. Science, 2017, 358, 768-771.	6.0	1,285

#	Article	IF	CITATIONS
37	Understanding the rate-dependent J–V hysteresis, slow time component, and aging in CH <sub>3</sub> NH <sub>3</sub> PbI <sub>3</sub> perovskite solar cells: the role of a compensated electric field. Energy and Environmental Science, 2015, 8, 995-1004.	15.6	1,150
38	Mixedâ€Organicâ€Cation Perovskite Photovoltaics for Enhanced Solarâ€Light Harvesting. Angewandte Chemie - International Edition, 2014, 53, 3151-3157.	7.2	1,117
39	Highly efficient planar perovskite solar cells through band alignment engineering. Energy and Environmental Science, 2015, 8, 2928-2934.	15.6	1,097
40	Entropic stabilization of mixed A-cation ABX <sub>3</sub> metal halide perovskites for high performance perovskite solar cells. Energy and Environmental Science, 2016, 9, 656-662.	15.6	1,077
41	Cation-Induced Band-Gap Tuning in Organohalide Perovskites: Interplay of Spin–Orbit Coupling and Octahedra Tilting. Nano Letters, 2014, 14, 3608-3616.	4.5	1,033
42	Improved performance and stability of perovskite solar cells by crystal crosslinking with alkylphosphonic acid ω-ammonium chlorides. Nature Chemistry, 2015, 7, 703-711.	6.6	1,033
43	Acidâ^'Base Equilibria of (2,2'-Bipyridyl-4,4'-dicarboxylic acid)ruthenium(II) Complexes and the Effect of Protonation on Charge-Transfer Sensitization of Nanocrystalline Titania. Inorganic Chemistry, 1999, 38, 6298-6305.	1.9	1,020
44	Materials interface engineering for solution-processed photovoltaics. Nature, 2012, 488, 304-312.	13.7	1,000
45	High-Efficiency Organic-Dye- Sensitized Solar Cells Controlled by Nanocrystalline-TiO2 Electrode Thickness. Advanced Materials, 2006, 18, 1202-1205.	11.1	997
46	Not All That Glitters Is Gold: Metal-Migration-Induced Degradation in Perovskite Solar Cells. ACS Nano, 2016, 10, 6306-6314.	7.3	966
47	Thermodynamically stabilized β-CsPbI <sub>3</sub> –based perovskite solar cells with efficiencies >18%. Science, 2019, 365, 591-595.	6.0	963
48	The rapid evolution of highly efficient perovskite solar cells. Energy and Environmental Science, 2017, 10, 710-727.	15.6	942
49	Towards stable and commercially available perovskite solar cells. Nature Energy, 2016, 1, .	19.8	941
50	Probing the photoelectrochemical properties of hematite (α-Fe <sub>2</sub> O <sub>3</sub> ) electrodes using hydrogen peroxide as a hole scavenger. Energy and Environmental Science, 2011, 4, 958-964.	15.6	933
51	Conformal quantum dot–SnO <sub>2</sub> layers as electron transporters for efficient perovskite solar cells. Science, 2022, 375, 302-306.	6.0	872
52	Dye-sensitized solar cells for efficient power generation under ambient lighting. Nature Photonics, 2017, 11, 372-378.	15.6	871
53	Photoelectrochemical Water Splitting with Mesoporous Hematite Prepared by a Solution-Based Colloidal Approach. Journal of the American Chemical Society, 2010, 132, 7436-7444.	6.6	865
54	Perovskite as Light Harvester: A Game Changer in Photovoltaics. Angewandte Chemie - International Edition, 2014, 53, 2812-2824.	7.2	862

#	Article	IF	CITATIONS
55	First-Principles Modeling of Mixed Halide Organometal Perovskites for Photovoltaic Applications. Journal of Physical Chemistry C, 2013, 117, 13902-13913.	1.5	861
56	Artificial photosynthesis. 1. Photosensitization of titania solar cells with chlorophyll derivatives and related natural porphyrins. The Journal of Physical Chemistry, 1993, 97, 6272-6277.	2.9	852
57	Effect of Annealing Temperature on Film Morphology of Organic–Inorganic Hybrid Pervoskite Solidâ€6tate Solar Cells. Advanced Functional Materials, 2014, 24, 3250-3258.	7.8	850
58	A molecularly engineered hole-transporting material for efficient perovskite solar cells. Nature Energy, 2016, 1, .	19.8	816
59	Subpicosecond Interfacial Charge Separation in Dye-Sensitized Nanocrystalline Titanium Dioxide Films. The Journal of Physical Chemistry, 1996, 100, 20056-20062.	2.9	815
60	Consensus statement for stability assessment and reporting for perovskite photovoltaics based on ISOS procedures. Nature Energy, 2020, 5, 35-49.	19.8	797
61	Holeâ€Transport Materials for Perovskite Solar Cells. Angewandte Chemie - International Edition, 2016, 55, 14522-14545.	7.2	786
62	Depleted-Heterojunction Colloidal Quantum Dot Solar Cells. ACS Nano, 2010, 4, 3374-3380.	7.3	781
63	Inorganic hole conductor-based lead halide perovskite solar cells with 12.4% conversion efficiency. Nature Communications, 2014, 5, 3834.	5.8	769
64	Passivating surface states on water splitting hematite photoanodes with alumina overlayers. Chemical Science, 2011, 2, 737-743.	3.7	763
65	Highly Efficient Mesoscopic Dye‧ensitized Solar Cells Based on Donor–Acceptor‧ubstituted Porphyrins. Angewandte Chemie - International Edition, 2010, 49, 6646-6649.	7.2	762
66	Improving efficiency and stability of perovskite solar cells with photocurable fluoropolymers. Science, 2016, 354, 203-206.	6.0	748
67	Enhanced electronic properties in mesoporous TiO2 via lithium doping for high-efficiency perovskite solar cells. Nature Communications, 2016, 7, 10379.	5.8	744
68	Highly efficient and stable planar perovskite solar cells by solution-processed tin oxide. Energy and Environmental Science, 2016, 9, 3128-3134.	15.6	720
69	Impedance Spectroscopic Analysis of Lead Iodide Perovskite-Sensitized Solid-State Solar Cells. ACS Nano, 2014, 8, 362-373.	7.3	663
70	Unravelling the mechanism of photoinduced charge transfer processes in lead iodide perovskite solar cells. Nature Photonics, 2014, 8, 250-255.	15.6	648
71	Semi-transparent perovskite solar cells for tandems with silicon and CIGS. Energy and Environmental Science, 2015, 8, 956-963.	15.6	630
72	Molecular Engineering of Organic Sensitizers for Dye-Sensitized Solar Cell Applications. Journal of the American Chemical Society, 2008, 130, 6259-6266.	6.6	625

#	Article	IF	CITATIONS
73	High-performance dye-sensitized solar cells based on solvent-free electrolytes produced from eutectic melts. Nature Materials, 2008, 7, 626-630.	13.3	622
74	Exploration of the compositional space for mixed lead halogen perovskites for high efficiency solar cells. Energy and Environmental Science, 2016, 9, 1706-1724.	15.6	622
75	A solvent- and vacuum-free route to large-area perovskite films for efficient solar modules. Nature, 2017, 550, 92-95.	13.7	618
76	Parameters Influencing Charge Recombination Kinetics in Dye-Sensitized Nanocrystalline Titanium Dioxide Films. Journal of Physical Chemistry B, 2000, 104, 538-547.	1.2	613
77	Ionic polarization-induced current–voltage hysteresis in CH3NH3PbX3 perovskite solar cells. Nature Communications, 2016, 7, 10334.	5.8	602
78	Influence of Feature Size, Film Thickness, and Silicon Doping on the Performance of Nanostructured Hematite Photoanodes for Solar Water Splitting. Journal of Physical Chemistry C, 2009, 113, 772-782.	1.5	594
79	Interpretation and evolution of open-circuit voltage, recombination, ideality factor and subgap defect states during reversible light-soaking and irreversible degradation of perovskite solar cells. Energy and Environmental Science, 2018, 11, 151-165.	15.6	586
80	Control of dark current in photoelectrochemical (TiO2/I––I3–) and dye-sensitized solar cells. Chemical Communications, 2005, , 4351.	2.2	561
81	Bication lead iodide 2D perovskite component to stabilize inorganic α-CsPbI <sub>3</sub> perovskite phase for high-efficiency solar cells. Science Advances, 2017, 3, e1700841.	4.7	557
82	A cobalt complex redox shuttle for dye-sensitized solar cells with high open-circuit potentials. Nature Communications, 2012, 3, 631.	5.8	554
83	Systematic investigation of the impact of operation conditions on the degradation behaviour of perovskite solar cells. Nature Energy, 2018, 3, 61-67.	19.8	544
84	Cu <sub>2</sub> O Nanowire Photocathodes for Efficient and Durable Solar Water Splitting. Nano Letters, 2016, 16, 1848-1857.	4.5	542
85	Monolithic perovskite/silicon-heterojunction tandem solar cells processed at low temperature. Energy and Environmental Science, 2016, 9, 81-88.	15.6	536
86	High efficiency stable inverted perovskite solar cells without current hysteresis. Energy and Environmental Science, 2015, 8, 2725-2733.	15.6	533
87	Vapor-assisted deposition of highly efficient, stable black-phase FAPbI <sub>3</sub> perovskite solar cells. Science, 2020, 370, .	6.0	530
88	Migration of cations induces reversible performance losses over day/night cycling in perovskite solar cells. Energy and Environmental Science, 2017, 10, 604-613.	15.6	525
89	Ultrahydrophobic 3D/2D fluoroarene bilayer-based water-resistant perovskite solar cells with efficiencies exceeding 22%. Science Advances, 2019, 5, eaaw2543.	4.7	524
90	An organic redox electrolyte to rival triiodide/iodide in dye-sensitized solar cells. Nature Chemistry, 2010, 2, 385-389.	6.6	510

#	Article	IF	CITATIONS
91	Thermal Behavior of Methylammonium Lead-Trihalide Perovskite Photovoltaic Light Harvesters. Chemistry of Materials, 2014, 26, 6160-6164.	3.2	502
92	Efficient Far Red Sensitization of Nanocrystalline TiO <sub>2</sub> Films by an Unsymmetrical Squaraine Dye. Journal of the American Chemical Society, 2007, 129, 10320-10321.	6.6	497
93	Boosting the performance of Cu2O photocathodes for unassisted solar water splitting devices. Nature Catalysis, 2018, 1, 412-420.	16.1	489
94	Pseudocapacitive Lithium Storage in TiO2(B). Chemistry of Materials, 2005, 17, 1248-1255.	3.2	467
95	WO <sub>3</sub> â^`Fe <sub>2</sub> O <sub>3</sub> Photoanodes for Water Splitting: A Host Scaffold, Guest Absorber Approach. Chemistry of Materials, 2009, 21, 2862-2867.	3.2	455
96	The Significance of Ion Conduction in a Hybrid Organic–Inorganic Leadâ€iodideâ€Based Perovskite Photosensitizer. Angewandte Chemie - International Edition, 2015, 54, 7905-7910.	7.2	447
97	Highly efficient water splitting by a dual-absorber tandem cell. Nature Photonics, 2012, 6, 824-828.	15.6	437
98	Solar conversion of CO2 to CO using Earth-abundant electrocatalysts prepared by atomic layer modification of CuO. Nature Energy, 2017, 2, .	19.8	436
99	Predicting the Openâ€Circuit Voltage of CH <sub>3</sub> NH <sub>3</sub> Pbl <sub>3</sub> Perovskite Solar Cells Using Electroluminescence and Photovoltaic Quantum Efficiency Spectra: the Role of Radiative and Nonâ€Radiative Recombination. Advanced Energy Materials, 2015, 5, 1400812.	10.2	425
100	Hydrogen evolution from a copper(I) oxide photocathode coated with an amorphous molybdenum sulphide catalyst. Nature Communications, 2014, 5, 3059.	5.8	418
101	Highly efficient semiconducting TiO2 photoelectrodes prepared by aerosol pyrolysis. Electrochimica Acta, 1995, 40, 643-652.	2.6	413
102	Dynamics of photogenerated holes in surface modified α-Fe <sub>2</sub> O <sub>3</sub> photoanodes for solar water splitting. Proceedings of the National Academy of Sciences of the United States of America, 2012, 109, 15640-15645.	3.3	413
103	Perovskite Solar Cells: From the Atomic Level to Film Quality and Device Performance. Angewandte Chemie - International Edition, 2018, 57, 2554-2569.	7.2	413
104	Large tunable photoeffect on ion conduction in halide perovskites and implications for photodecomposition. Nature Materials, 2018, 17, 445-449.	13.3	410
105	Significant Improvement of Dyeâ€Sensitized Solar Cell Performance by Small Structural Modification in Ï€â€Conjugated Donor–Acceptor Dyes. Advanced Functional Materials, 2012, 22, 1291-1302.	7.8	404
106	Coll(dbbip)22+ Complex Rivals Tri-iodide/Iodide Redox Mediator in Dye-Sensitized Photovoltaic Cells. Journal of Physical Chemistry B, 2001, 105, 10461-10464.	1.2	402
107	Ultrathin films on copper(i) oxide water splitting photocathodes: a study on performance and stability. Energy and Environmental Science, 2012, 5, 8673.	15.6	401
108	Nanocrystalline Rutile Electron Extraction Layer Enables Low-Temperature Solution Processed Perovskite Photovoltaics with 13.7% Efficiency. Nano Letters, 2014, 14, 2591-2596.	4.5	397

#	Article	IF	CITATIONS
109	Back Electron–Hole Recombination in Hematite Photoanodes for Water Splitting. Journal of the American Chemical Society, 2014, 136, 2564-2574.	6.6	393
110	Electrodeposited Nanocomposite n-p Heterojunctions for Solid-State Dye-Sensitized Photovoltaics. Advanced Materials, 2000, 12, 1263-1267.	11.1	392
111	Europium-Doped CsPbl2Br for Stable and Highly Efficient Inorganic Perovskite Solar Cells. Joule, 2019, 3, 205-214.	11.7	387
112	The synergistic effect of H <sub>2</sub> O and DMF towards stable and 20% efficiency inverted perovskite solar cells. Energy and Environmental Science, 2017, 10, 808-817.	15.6	383
113	A Simple 3,4â€Ethylenedioxythiophene Based Holeâ€Transporting Material for Perovskite Solar Cells. Angewandte Chemie - International Edition, 2014, 53, 4085-4088.	7.2	379
114	A low-cost spiro[fluorene-9,9′-xanthene]-based hole transport material for highly efficient solid-state dye-sensitized solar cells and perovskite solar cells. Energy and Environmental Science, 2016, 9, 873-877.	15.6	362
115	Controlling Photoactivity in Ultrathin Hematite Films for Solar Waterâ€Splitting. Advanced Functional Materials, 2010, 20, 1099-1107.	7.8	357
116	Diffusion engineering of ions and charge carriers for stable efficient perovskite solar cells. Nature Communications, 2017, 8, 15330.	5.8	356
117	Graphene Nanoplatelets Outperforming Platinum as the Electrocatalyst in Co-Bipyridine-Mediated Dye-Sensitized Solar Cells. Nano Letters, 2011, 11, 5501-5506.	4.5	350
118	Cooperative Effect of Adsorbed Cations and Iodide on the Interception of Back Electron Transfer in the Dye Sensitization of Nanocrystalline TiO2. Journal of Physical Chemistry B, 2000, 104, 1791-1795.	1.2	341
119	Self-Organization of TiO2Nanoparticles in Thin Films. Chemistry of Materials, 1998, 10, 2419-2425.	3.2	334
120	High-Efficiency and Stable Mesoscopic Dye-Sensitized Solar Cells Based on a High Molar Extinction Coefficient Ruthenium Sensitizer and Nonvolatile Electrolyte. Advanced Materials, 2007, 19, 1133-1137.	11.1	332
121	Cyclopentadithiophene Bridged Donor–Acceptor Dyes Achieve High Power Conversion Efficiencies in Dye‧ensitized Solar Cells Based on the <i>tris</i> â€Cobalt Bipyridine Redox Couple. ChemSusChem, 2011, 4, 591-594.	3.6	327
122	Triazatruxene-Based Hole Transporting Materials for Highly Efficient Perovskite Solar Cells. Journal of the American Chemical Society, 2015, 137, 16172-16178.	6.6	321
123	Isomerâ€Pure Bisâ€PCBMâ€Assisted Crystal Engineering of Perovskite Solar Cells Showing Excellent Efficiency and Stability. Advanced Materials, 2017, 29, 1606806.	11.1	320
124	Panchromatic engineering for dye-sensitized solar cells. Energy and Environmental Science, 2011, 4, 842-857.	15.6	319
125	Phase Segregation in Cs-, Rb- and K-Doped Mixed-Cation (MA) <sub><i>x</i></sub> (FA) <sub>1–<i>x</i></sub> Pbl <sub>3</sub> Hybrid Perovskites from Solid-State NMR. Journal of the American Chemical Society, 2017, 139, 14173-14180.	6.6	317
126	The Transient Photocurrent and Photovoltage Behavior of a Hematite Photoanode under Working Conditions and the Influence of Surface Treatments. Journal of Physical Chemistry C, 2012, 116, 26707-26720.	1.5	315

#	Article	IF	CITATIONS
127	Methodologies toward Highly Efficient Perovskite Solar Cells. Small, 2018, 14, e1704177.	5.2	315
128	Origin of unusual bandgap shift and dual emission in organic-inorganic lead halide perovskites. Science Advances, 2016, 2, e1601156.	4.7	307
129	Synthesis and Characterization of High-Photoactivity Electrodeposited Cu <sub>2</sub> O Solar Absorber by Photoelectrochemistry and Ultrafast Spectroscopy. Journal of Physical Chemistry C, 2012, 116, 7341-7350.	1.5	305
130	Tailored Amphiphilic Molecular Mitigators for Stable Perovskite Solar Cells with 23.5% Efficiency. Advanced Materials, 2020, 32, e1907757.	11.1	303
131	Nanostructured TiO2/CH3NH3PbI3 heterojunction solar cells employing spiro-OMeTAD/Co-complex as hole-transporting material. Journal of Materials Chemistry A, 2013, 1, 11842.	5.2	301
132	Efficient photosynthesis of carbon monoxide from CO2 using perovskite photovoltaics. Nature Communications, 2015, 6, 7326.	5.8	295
133	Real-space observation of unbalanced charge distribution inside a perovskite-sensitized solar cell. Nature Communications, 2014, 5, 5001.	5.8	294
134	Direct Contact of Selective Charge Extraction Layers Enables High-Efficiency Molecular Photovoltaics. Joule, 2018, 2, 1108-1117.	11.7	291
135	Decoupling Feature Size and Functionality in Solution-Processed, Porous Hematite Electrodes for Solar Water Splitting. Nano Letters, 2010, 10, 4155-4160.	4.5	290
136	Understanding the Role of Underlayers and Overlayers in Thin Film Hematite Photoanodes. Advanced Functional Materials, 2014, 24, 7681-7688.	7.8	289
137	How the formation of interfacial charge causes hysteresis in perovskite solar cells. Energy and Environmental Science, 2018, 11, 2404-2413.	15.6	289
138	Identifying and suppressing interfacial recombination to achieve high open-circuit voltage in perovskite solar cells. Energy and Environmental Science, 2017, 10, 1207-1212.	15.6	288
139	Preparation of TiO2 (anatase) films on electrodes by anodic oxidative hydrolysis of TiCl3. Journal of Electroanalytical Chemistry, 1993, 346, 291-307.	1.9	283
140	Slow cooling and highly efficient extraction of hot carriers in colloidal perovskite nanocrystals. Nature Communications, 2017, 8, 14350.	5.8	282
141	The Rise of Highly Efficient and Stable Perovskite Solar Cells. Accounts of Chemical Research, 2017, 50, 487-491.	7.6	282
142	Enhancing Efficiency of Perovskite Solar Cells via Nâ€doped Graphene: Crystal Modification and Surface Passivation. Advanced Materials, 2016, 28, 8681-8686.	11.1	281
143	Insight into D–Aâ~ï€â€"A Structured Sensitizers: A Promising Route to Highly Efficient and Stable Dye-Sensitized Solar Cells. ACS Applied Materials & Interfaces, 2015, 7, 9307-9318.	4.0	278
144	Suppressing defects through the synergistic effect of a Lewis base and a Lewis acid for highly efficient and stable perovskite solar cells. Energy and Environmental Science, 2018, 11, 3480-3490.	15.6	274

#	Article	IF	CITATIONS
145	Rate Law Analysis of Water Oxidation on a Hematite Surface. Journal of the American Chemical Society, 2015, 137, 6629-6637.	6.6	273
146	Covalent Immobilization of a Molecular Catalyst on Cu <sub>2</sub> O Photocathodes for CO <sub>2</sub> Reduction. Journal of the American Chemical Society, 2016, 138, 1938-1946.	6.6	272
147	Enhancement in the Performance of Ultrathin Hematite Photoanode for Water Splitting by an Oxide Underlayer. Advanced Materials, 2012, 24, 2699-2702.	11.1	271
148	Gallium arsenide p-i-n radial structures for photovoltaic applications. Applied Physics Letters, 2009, 94, .	1.5	270
149	A Stable Blue Photosensitizer for Color Palette of Dye-Sensitized Solar Cells Reaching 12.6% Efficiency. Journal of the American Chemical Society, 2018, 140, 2405-2408.	6.6	270
150	Selective C–C Coupling in Carbon Dioxide Electroreduction via Efficient Spillover of Intermediates As Supported by Operando Raman Spectroscopy. Journal of the American Chemical Society, 2019, 141, 18704-18714.	6.6	270
151	The Role of Surface States in the Ultrafast Photoinduced Electron Transfer from Sensitizing Dye Molecules to Semiconductor Colloids. Journal of Physical Chemistry B, 2000, 104, 8995-9003.	1.2	269
152	Cathodic shift in onset potential of solar oxygen evolution on hematite by 13-group oxide overlayers. Energy and Environmental Science, 2011, 4, 2512.	15.6	269
153	Atomic-level passivation mechanism of ammonium salts enabling highly efficient perovskite solar cells. Nature Communications, 2019, 10, 3008.	5.8	268
154	Multifunctional molecular modulators for perovskite solar cells with over 20% efficiency and high operational stability. Nature Communications, 2018, 9, 4482.	5.8	266
155	Recent developments in redox electrolytes for dye-sensitized solar cells. Energy and Environmental Science, 2012, 5, 9394.	15.6	265
156	Dynamics of photogenerated holes in nanocrystalline α-Fe <sub>2</sub> O <sub>3</sub> electrodes for water oxidation probed by transient absorption spectroscopy. Chemical Communications, 2011, 47, 716-718.	2.2	261
157	Optimization of distyryl-Bodipy chromophores for efficient panchromatic sensitization in dye sensitized solar cells. Chemical Science, 2011, 2, 949.	3.7	259
158	Nanocrystalline Mesoporous Strontium Titanate as Photoelectrode Material for Photosensitized Solar Devices:  Increasing Photovoltage through Flatband Potential Engineering. Journal of Physical Chemistry B, 1999, 103, 9328-9332.	1.2	258
159	Highâ€Performance Perovskite Solar Cells with Enhanced Environmental Stability Based on Amphiphileâ€Modified CH <sub>3</sub> NH <sub>3</sub> PbI <sub>3</sub> . Advanced Materials, 2016, 28, 2910-2915.	11.1	258
160	Dye Dependent Regeneration Dynamics in Dye Sensitized Nanocrystalline Solar Cells:  Evidence for the Formation of a Ruthenium Bipyridyl Cation/Iodide Intermediate. Journal of Physical Chemistry C, 2007, 111, 6561-6567.	1.5	257
161	Alkyl Chain Barriers for Kinetic Optimization in Dye-Sensitized Solar Cells. Journal of the American Chemical Society, 2006, 128, 16376-16383.	6.6	254
162	The 2,2,6,6â€Tetramethylâ€1â€piperidinyloxy Radical: An Efficient, Iodine―Free Redox Mediator for Dyeâ€Sensitized Solar Cells. Advanced Functional Materials, 2008, 18, 341-346.	7.8	254

#	Article	IF	CITATIONS
163	Ruthenium Oxide Hydrogen Evolution Catalysis on Composite Cuprous Oxide Water‧plitting Photocathodes. Advanced Functional Materials, 2014, 24, 303-311.	7.8	253
164	Facile synthesized organic hole transporting material for perovskite solar cell with efficiency of 19.8%. Nano Energy, 2016, 23, 138-144.	8.2	253
165	An Optically Transparent Iron Nickel Oxide Catalyst for Solar Water Splitting. Journal of the American Chemical Society, 2015, 137, 9927-9936.	6.6	247
166	Enhanced charge carrier mobility and lifetime suppress hysteresis and improve efficiency in planar perovskite solar cells. Energy and Environmental Science, 2018, 11, 78-86.	15.6	246
167	Unbroken Perovskite: Interplay of Morphology, Electroâ€optical Properties, and Ionic Movement. Advanced Materials, 2016, 28, 5031-5037.	11.1	242
168	The effect of illumination on the formation of metal halide perovskite films. Nature, 2017, 545, 208-212.	13.7	242
169	Real-Time Observation of Photoinduced Adiabatic Electron Transfer in Strongly Coupled Dye/Semiconductor Colloidal Systems with a 6 fs Time Constant. Journal of Physical Chemistry B, 2002, 106, 6494-6499.	1.2	239
170	A Methoxydiphenylamine‧ubstituted Carbazole Twin Derivative: An Efficient Hole‶ransporting Material for Perovskite Solar Cells. Angewandte Chemie - International Edition, 2015, 54, 11409-11413.	7.2	239
171	Copper Bipyridyl Redox Mediators for Dye-Sensitized Solar Cells with High Photovoltage. Journal of the American Chemical Society, 2016, 138, 15087-15096.	6.6	239
172	New Strategies for Defect Passivation in Highâ€Efficiency Perovskite Solar Cells. Advanced Energy Materials, 2020, 10, 1903090.	10.2	237
173	Formation of Stable Mixed Guanidinium–Methylammonium Phases with Exceptionally Long Carrier Lifetimes for High-Efficiency Lead Iodide-Based Perovskite Photovoltaics. Journal of the American Chemical Society, 2018, 140, 3345-3351.	6.6	235
174	Over 20% PCE perovskite solar cells with superior stability achieved by novel and low-cost hole-transporting materials. Nano Energy, 2017, 41, 469-475.	8.2	232
175	11% efficiency solid-state dye-sensitized solar cells with copper(II/I) hole transport materials. Nature Communications, 2017, 8, 15390.	5.8	229
176	A Smooth CH <sub>3</sub> NH <sub>3</sub> PbI <sub>3</sub> Film via a New Approach for Forming the PbI <sub>2</sub> Nanostructure Together with Strategically High CH <sub>3</sub> NH <sub>3</sub> I Concentration for High Efficient Planarâ€Heterojunction Solar Cells. Advanced Energy Materials, 2015, 5, 1501354.	10.2	228
177	A Bismuth Vanadate–Cuprous Oxide Tandem Cell for Overall Solar Water Splitting. Journal of Physical Chemistry C, 2014, 118, 16959-16966.	1.5	226
178	Influence of Ancillary Ligands in Dye-Sensitized Solar Cells. Chemical Reviews, 2016, 116, 9485-9564.	23.0	225
179	Ionic Liquid Control Crystal Growth to Enhance Planar Perovskite Solar Cells Efficiency. Advanced Energy Materials, 2016, 6, 1600767.	10.2	224
180	Solutionâ€Processed Tinâ€Based Perovskite for Nearâ€Infrared Lasing. Advanced Materials, 2016, 28, 8191-8196.	11.1	222

#	Article	IF	CITATIONS
181	Bifunctional Organic Spacers for Formamidinium-Based Hybrid Dion–Jacobson Two-Dimensional Perovskite Solar Cells. Nano Letters, 2019, 19, 150-157.	4.5	218
182	Modification of TiO2 Heterojunctions with Benzoic Acid Derivatives in Hybrid Molecular Solid-State Devices. Advanced Materials, 2000, 12, 447-451.	11.1	216
183	Improvement of the photovoltaic performance of solid-state dye-sensitized device by silver complexation of the sensitizer cis-bis(4,4′-dicarboxy-2,2′bipyridine)-bis(isothiocyanato) ruthenium(II). Applied Physics Letters, 2002, 81, 367-369.	1.5	216
184	Novel p-dopant toward highly efficient and stable perovskite solar cells. Energy and Environmental Science, 2018, 11, 2985-2992.	15.6	216
185	Inverted Current–Voltage Hysteresis in Mixed Perovskite Solar Cells: Polarization, Energy Barriers, and Defect Recombination. Advanced Energy Materials, 2016, 6, 1600396.	10.2	213
186	The Nature of Ion Conduction in Methylammonium Lead Iodide: A Multimethod Approach. Angewandte Chemie - International Edition, 2017, 56, 7755-7759.	7.2	213
187	High Temperatureâ€Stable Perovskite Solar Cell Based on Lowâ€Cost Carbon Nanotube Hole Contact. Advanced Materials, 2017, 29, 1606398.	11.1	209
188	Cation Dynamics in Mixed-Cation (MA) <sub><i>x</i></sub> (FA) <sub>1–<i>x</i></sub> PbI <sub>3</sub> Hybrid Perovskites from Solid-State NMR. Journal of the American Chemical Society, 2017, 139, 10055-10061.	6.6	209
189	Dye-sensitized solar cells based on poly (3,4-ethylenedioxythiophene) counter electrode derived from ionic liquids. Journal of Materials Chemistry, 2010, 20, 1654.	6.7	208
190	A simple spiro-type hole transporting material for efficient perovskite solar cells. Energy and Environmental Science, 2015, 8, 1986-1991.	15.6	206
191	Light Harvesting and Charge Recombination in CH <sub>3</sub> NH <sub>3</sub> PbI <sub>3</sub> Perovskite Solar Cells Studied by Hole Transport Layer Thickness Variation. ACS Nano, 2015, 9, 4200-4209.	7.3	205
192	Cobalt Electrolyte/Dye Interactions in Dye-Sensitized Solar Cells: A Combined Computational and Experimental Study. Journal of the American Chemical Society, 2012, 134, 19438-19453.	6.6	204
193	Mesoporous SnO2 electron selective contact enables UV-stable perovskite solar cells. Nano Energy, 2016, 30, 517-522.	8.2	204
194	A dopant free linear acene derivative as a hole transport material for perovskite pigmented solar cells. Energy and Environmental Science, 2015, 8, 1816-1823.	15.6	202
195	Electrochemical Characterization of TiO <sub>2</sub> Blocking Layers for Dye-Sensitized Solar Cells. Journal of Physical Chemistry C, 2014, 118, 16408-16418.	1.5	201
196	A Power Pack Based on Organometallic Perovskite Solar Cell and Supercapacitor. ACS Nano, 2015, 9, 1782-1787.	7.3	201
197	Stabilization of Highly Efficient and Stable Phaseâ€Pure FAPbl <sub>3</sub> Perovskite Solar Cells by Molecularly Tailored 2Dâ€Overlayers. Angewandte Chemie - International Edition, 2020, 59, 15688-15694.	7.2	201
198	Efficient co-sensitization of nanocrystalline TiO2 films by organic sensitizers. Chemical Communications, 2007, , 4680.	2.2	198

#	Article	IF	CITATIONS
199	Molecular Design of Unsymmetrical Squaraine Dyes for High Efficiency Conversion of Low Energy Photons into Electrons Using TiO <sub>2</sub> Nanocrystalline Films. Advanced Functional Materials, 2009, 19, 2720-2727.	7.8	197
200	Influence of the interfacial charge-transfer resistance at the counter electrode in dye-sensitized solar cells employing cobalt redox shuttles. Energy and Environmental Science, 2011, 4, 4921.	15.6	196
201	Impact of Monovalent Cation Halide Additives on the Structural and Optoelectronic Properties of CH <sub>3</sub> NH <sub>3</sub> PbI <sub>3</sub> Perovskite. Advanced Energy Materials, 2016, 6, 1502472.	10.2	196
202	A molecular photosensitizer achieves a Voc of 1.24 V enabling highly efficient and stable dye-sensitized solar cells with copper(II/I)-based electrolyte. Nature Communications, 2021, 12, 1777.	5.8	196
203	The Function of a TiO <sub>2</sub> Compact Layer in Dye-Sensitized Solar Cells Incorporating "Planar― Organic Dyes. Nano Letters, 2008, 8, 977-981.	4.5	195
204	Efficient and stable inverted perovskite solar cells with very high fill factors via incorporation of star-shaped polymer. Science Advances, 2021, 7, .	4.7	195
205	Photoelectrocatalytic arene C–H amination. Nature Catalysis, 2019, 2, 366-373.	16.1	193
206	In situ dynamic observations of perovskite crystallisation and microstructure evolution intermediated from [PbI6]4â° cage nanoparticles. Nature Communications, 2017, 8, 15688.	5.8	191
207	Synergistic Crystal and Interface Engineering for Efficient and Stable Perovskite Photovoltaics. Advanced Energy Materials, 2019, 9, 1802646.	10.2	189
208	Multihole water oxidation catalysis on haematite photoanodes revealed by operando spectroelectrochemistry and DFT. Nature Chemistry, 2020, 12, 82-89.	6.6	189
209	Subnanometer Ga <sub>2</sub> O <sub>3</sub> Tunnelling Layer by Atomic Layer Deposition to Achieve 1.1 V Open-Circuit Potential in Dye-Sensitized Solar Cells. Nano Letters, 2012, 12, 3941-3947.	4.5	188
210	Benzotrithiopheneâ€Based Holeâ€Transporting Materials for 18.2 % Perovskite Solar Cells. Angewandte Chemie - International Edition, 2016, 55, 6270-6274.	7.2	188
211	Performance of perovskite solar cells under simulated temperature-illumination real-world operating conditions. Nature Energy, 2019, 4, 568-574.	19.8	186
212	Investigation Regarding the Role of Chloride in Organic–Inorganic Halide Perovskites Obtained from Chloride Containing Precursors. Nano Letters, 2014, 14, 6991-6996.	4.5	185
213	A quasi core–shell nitrogen-doped graphene/cobalt sulfide conductive catalyst for highly efficient dye-sensitized solar cells. Energy and Environmental Science, 2014, 7, 2637-2641.	15.6	185
214	Carbon nanotube-based hybrid hole-transporting material and selective contact for high efficiency perovskite solar cells. Energy and Environmental Science, 2016, 9, 461-466.	15.6	185
215	Improving the stability and performance of perovskite solar cells <i>via</i> off-the-shelf post-device ligand treatment. Energy and Environmental Science, 2018, 11, 2253-2262.	15.6	181
216	Transforming Hybrid Organic Inorganic Perovskites by Rapid Halide Exchange. Chemistry of Materials, 2015, 27, 2181-2188.	3.2	179

#	Article	IF	CITATIONS
217	Toward All Roomâ€Temperature, Solutionâ€Processed, Highâ€Performance Planar Perovskite Solar Cells: A New Scheme of Pyridineâ€Promoted Perovskite Formation. Advanced Materials, 2017, 29, 1604695.	11.1	178
218	Giant five-photon absorption from multidimensional core-shell halide perovskite colloidal nanocrystals. Nature Communications, 2017, 8, 15198.	5.8	177
219	Chemical Distribution of Multiple Cation (Rb <sup>+</sup> , Cs <sup>+</sup> , MA <sup>+</sup> , and) Tj ETQq1 1 29, 3589-3596.	0.784314 3.2	ł rgBT /Overl 175
220	Co(III) Complexes as p-Dopants in Solid-State Dye-Sensitized Solar Cells. Chemistry of Materials, 2013, 25, 2986-2990.	3.2	169
221	First Principles Design of Dye Molecules with Ullazine Donor for Dye Sensitized Solar Cells. Journal of Physical Chemistry C, 2013, 117, 3772-3778.	1.5	169
222	A swivel-cruciform thiophene based hole-transporting material for efficient perovskite solar cells. Journal of Materials Chemistry A, 2014, 2, 6305-6309.	5.2	167
223	Efficient Perovskite Solar Cell Modules with High Stability Enabled by Iodide Diffusion Barriers. Joule, 2019, 3, 2748-2760.	11.7	167
224	High-Efficiency Polycrystalline Thin Film Tandem Solar Cells. Journal of Physical Chemistry Letters, 2015, 6, 2676-2681.	2.1	166
225	Silolothiophene-linked triphenylamines as stable hole transporting materials for high efficiency perovskite solar cells. Energy and Environmental Science, 2015, 8, 2946-2953.	15.6	163
226	Mechanosynthesis of the hybrid perovskite CH <sub>3</sub> NH <sub>3</sub> PbI <sub>3</sub> : characterization and the corresponding solar cell efficiency. Journal of Materials Chemistry A, 2015, 3, 20772-20777.	5.2	163
227	Novel nanostructures for next generation dye-sensitized solar cells. Energy and Environmental Science, 2012, 5, 8506.	15.6	162
228	Hematite photoelectrodes for water splitting: evaluation of the role of film thickness by impedance spectroscopy. Physical Chemistry Chemical Physics, 2014, 16, 16515.	1.3	162
229	A Novel Dopantâ€Free Triphenylamine Based Molecular "Butterfly―Holeâ€Transport Material for Highly Efficient and Stable Perovskite Solar Cells. Advanced Energy Materials, 2016, 6, 1600401.	10.2	161
230	Enhanced Efficiency and Stability of Perovskite Solar Cells Through Ndâ€Đoping of Mesostructured TiO <sub>2</sub> . Advanced Energy Materials, 2016, 6, 1501868.	10.2	157
231	Low-Temperature Nb-Doped SnO <sub>2</sub> Electron-Selective Contact Yields over 20% Efficiency in Planar Perovskite Solar Cells. ACS Energy Letters, 2018, 3, 773-778.	8.8	157
232	Bipolar Membraneâ€Assisted Solar Water Splitting in Optimal pH. Advanced Energy Materials, 2016, 6, 1600100.	10.2	156
233	Regeneration and recombination kinetics in cobalt polypyridine based dye-sensitized solar cells, explained using Marcus theory. Physical Chemistry Chemical Physics, 2013, 15, 7087.	1.3	153
234	Enhanced Charge Collection with Passivation Layers in Perovskite Solar Cells. Advanced Materials, 2016, 28, 3966-3972.	11,1	152

#	Article	IF	CITATIONS
235	Synergistic Effect of Fluorinated Passivator and Hole Transport Dopant Enables Stable Perovskite Solar Cells with an Efficiency Near 24%. Journal of the American Chemical Society, 2021, 143, 3231-3237.	6.6	152
236	Atomic Layer Deposition of ZnO on CuO Enables Selective and Efficient Electroreduction of Carbon Dioxide to Liquid Fuels. Angewandte Chemie - International Edition, 2019, 58, 15036-15040.	7.2	150
237	Transparent Cuprous Oxide Photocathode Enabling a Stacked Tandem Cell for Unbiased Water Splitting. Advanced Energy Materials, 2015, 5, 1501537.	10.2	149
238	Subâ€Nanometer Conformal TiO <sub>2</sub> Blocking Layer for High Efficiency Solidâ€State Perovskite Absorber Solar Cells. Advanced Materials, 2014, 26, 4309-4312.	11.1	148
239	Comprehensive control of voltage loss enables 11.7% efficient solid-state dye-sensitized solar cells. Energy and Environmental Science, 2018, 11, 1779-1787.	15.6	148
240	High Molar Extinction Coefficient Ion-Coordinating Ruthenium Sensitizer for Efficient and Stable Mesoscopic Dye-Sensitized Solar Cells. Advanced Functional Materials, 2007, 17, 154-160.	7.8	147
241	Highly Efficient Perovskite Solar Cells with Gradient Bilayer Electron Transport Materials. Nano Letters, 2018, 18, 3969-3977.	4.5	147
242	Crown Ether Modulation Enables over 23% Efficient Formamidinium-Based Perovskite Solar Cells. Journal of the American Chemical Society, 2020, 142, 19980-19991.	6.6	145
243	Perovskite Photovoltaics with Outstanding Performance Produced by Chemical Conversion of Bilayer Mesostructured Lead Halide/TiO <sub>2</sub> Films. Advanced Materials, 2016, 28, 2964-2970.	11.1	144
244	Effect of Sensitizer Adsorption Temperature on the Performance of Dye-Sensitized Solar Cells. Journal of the American Chemical Society, 2011, 133, 9304-9310.	6.6	143
245	Blue-Coloured Highly Efficient Dye-Sensitized Solar Cells by Implementing the Diketopyrrolopyrrole Chromophore. Scientific Reports, 2013, 3, 2446.	1.6	143
246	Efficient and selective carbon dioxide reduction on low cost protected Cu <sub>2</sub> 0 photocathodes using a molecular catalyst. Energy and Environmental Science, 2015, 8, 855-861.	15.6	142
247	Copper Phenanthroline as a Fast and High-Performance Redox Mediator for Dye-Sensitized Solar Cells. Journal of Physical Chemistry C, 2016, 120, 9595-9603.	1.5	140
248	Interaction of oxygen with halide perovskites. Journal of Materials Chemistry A, 2018, 6, 10847-10855.	5.2	140
249	Holeâ€Transporting Small Molecules Based on Thiophene Cores for High Efficiency Perovskite Solar Cells. ChemSusChem, 2014, 7, 3420-3425.	3.6	139
250	Cu2O photocathodes with band-tail states assisted hole transport for standalone solar water splitting. Nature Communications, 2020, 11, 318.	5.8	139
251	Branched methoxydiphenylamine-substituted fluorene derivatives as hole transporting materials for high-performance perovskite solar cells. Energy and Environmental Science, 2016, 9, 1681-1686.	15.6	138
252	Direct Observation of Two Electron Holes in a Hematite Photoanode during Photoelectrochemical Water Splitting. Journal of Physical Chemistry C, 2012, 116, 16870-16875.	1.5	137

#	Article	IF	CITATIONS
253	Air Processed Inkjet Infiltrated Carbon Based Printed Perovskite Solar Cells with High Stability and Reproducibility. Advanced Materials Technologies, 2017, 2, 1600183.	3.0	137
254	Addition of adamantylammonium iodide to hole transport layers enables highly efficient and electroluminescent perovskite solar cells. Energy and Environmental Science, 2018, 11, 3310-3320.	15.6	137
255	Cobalt Redox Mediators for Ruthenium-Based Dye-Sensitized Solar Cells: A Combined Impedance Spectroscopy and Near-IR Transmittance Study. Journal of Physical Chemistry C, 2011, 115, 18847-18855.	1.5	136
256	Valence and conduction band tuning in halide perovskites for solar cell applications. Journal of Materials Chemistry A, 2016, 4, 15997-16002.	5.2	132
257	Light-induced reactivity of gold and hybrid perovskite as a new possible degradation mechanism in perovskite solar cells. Journal of Materials Chemistry A, 2018, 6, 1780-1786.	5.2	132
258	A dopant-free spirobi[cyclopenta[2,1-b:3,4-b′]dithiophene] based hole-transport material for efficient perovskite solar cells. Materials Horizons, 2015, 2, 613-618.	6.4	131
259	The Effect of Hole Transport Material Pore Filling on Photovoltaic Performance in Solidâ€State Dyeâ€Sensitized Solar Cells. Advanced Energy Materials, 2011, 1, 407-414.	10.2	130
260	Effect of Cation Composition on the Mechanical Stability of Perovskite Solar Cells. Advanced Energy Materials, 2018, 8, 1702116.	10.2	130
261	Phase Segregation in Potassium-Doped Lead Halide Perovskites from <sup>39</sup> K Solid-State NMR at 21.1 T. Journal of the American Chemical Society, 2018, 140, 7232-7238.	6.6	130
262	High-performance pure blue phosphorescent OLED using a novel bis-heteroleptic iridium(iii) complex with fluorinated bipyridyl ligands. Journal of Materials Chemistry C, 2013, 1, 1070.	2.7	129
263	Working Principles of Perovskite Photodetectors: Analyzing the Interplay Between Photoconductivity and Voltageâ€Driven Energyâ€Level Alignment. Advanced Functional Materials, 2015, 25, 6936-6947.	7.8	129
264	Identifying Fundamental Limitations in Halide Perovskite Solar Cells. Advanced Materials, 2016, 28, 2439-2445.	11.1	129
265	On the Solar to Hydrogen Conversion Efficiency of Photoelectrodes for Water Splitting. Journal of Physical Chemistry Letters, 2014, 5, 3330-3334.	2.1	128
266	Low band gap S,N-heteroacene-based oligothiophenes as hole-transporting and light absorbing materials for efficient perovskite-based solar cells. Energy and Environmental Science, 2014, 7, 2981.	15.6	127
267	Crystal Structure of DMF-Intermediate Phases Uncovers the Link Between CH <sub>3</sub> NH <sub>3</sub> PbI <sub>3</sub> Morphology and Precursor Stoichiometry. Journal of Physical Chemistry C, 2017, 121, 20739-20743.	1.5	126
268	Kinetics of Photoelectrochemical Oxidation of Methanol on Hematite Photoanodes. Journal of the American Chemical Society, 2017, 139, 11537-11543.	6.6	125
269	Impact of Peripheral Groups on Phenothiazine-Based Hole-Transporting Materials for Perovskite Solar Cells. ACS Energy Letters, 2018, 3, 1145-1152.	8.8	125
270	Guanidiniumâ€Assisted Surface Matrix Engineering for Highly Efficient Perovskite Quantum Dot Photovoltaics. Advanced Materials, 2020, 32, e2001906.	11.1	125

#	Article	IF	CITATIONS
271	Roomâ€Temperature Formation of Highly Crystalline Multication Perovskites for Efficient, Low ost Solar Cells. Advanced Materials, 2017, 29, 1606258.	11.1	124
272	Transparent, Conducting Nb:SnO <sub>2</sub> for Host–Guest Photoelectrochemistry. Nano Letters, 2012, 12, 5431-5435.	4.5	122
273	Spectral splitting photovoltaics using perovskite and wideband dye-sensitized solar cells. Nature Communications, 2015, 6, 8834.	5.8	122
274	The Role of Rubidium in Multiple ationâ€Based Highâ€Efficiency Perovskite Solar Cells. Advanced Materials, 2017, 29, 1701077.	11.1	120
275	Flexible perovskite solar cells with simultaneously improved efficiency, operational stability, and mechanical reliability. Joule, 2021, 5, 1587-1601.	11.7	120
276	Ultrathin Buffer Layers of SnO <sub>2</sub> by Atomic Layer Deposition: Perfect Blocking Function and Thermal Stability. Journal of Physical Chemistry C, 2017, 121, 342-350.	1.5	118
277	Largeâ€Grain Tinâ€Rich Perovskite Films for Efficient Solar Cells via Metal Alloying Technique. Advanced Materials, 2018, 30, 1705998.	11.1	116
278	Mesoscopic Oxide Double Layer as Electron Specific Contact for Highly Efficient and UV Stable Perovskite Photovoltaics. Nano Letters, 2018, 18, 2428-2434.	4.5	116
279	Charge extraction via graded doping of hole transport layers gives highly luminescent and stable metal halide perovskite devices. Science Advances, 2019, 5, eaav2012.	4.7	116
280	Catechol as an efficient anchoring group for attachment of ruthenium–polypyridine photosensitisers to solar cells based on nanocrystalline TiO2 films. New Journal of Chemistry, 2000, 24, 651-652.	1.4	115
281	Boosting the Efficiency of Perovskite Solar Cells with CsBrâ€Modified Mesoporous TiO <sub>2</sub> Beads as Electronâ€Selective Contact. Advanced Functional Materials, 2018, 28, 1705763.	7.8	115
282	Modulation of perovskite crystallization processes towards highly efficient and stable perovskite solar cells with MXene quantum dot-modified SnO <sub>2</sub> . Energy and Environmental Science, 2021, 14, 3447-3454.	15.6	115
283	Interfacial Passivation Engineering of Perovskite Solar Cells with Fill Factor over 82% and Outstanding Operational Stability on n-i-p Architecture. ACS Energy Letters, 2021, 6, 3916-3923.	8.8	115
284	Stabilization of the Perovskite Phase of Formamidinium Lead Triiodide by Methylammonium, Cs, and/or Rb Doping. Journal of Physical Chemistry Letters, 2017, 8, 1191-1196.	2.1	114
285	Facile route to freestanding CH3NH3PbI3 crystals using inverse solubility. Scientific Reports, 2015, 5, 11654.	1.6	112
286	Improved environmental stability of organic lead trihalide perovskite-based photoactive-layers in the presence of mesoporous TiO <sub>2</sub> . Journal of Materials Chemistry A, 2015, 3, 7219-7223.	5.2	112
287	Targeting Ideal Dualâ€Absorber Tandem Water Splitting Using Perovskite Photovoltaics and Culn <i><sub>x</sub></i> Ga <sub>1â€<i>x</i></sub> Se <sub>2</sub> Photocathodes. Advanced Energy Materials, 2015, 5, 1501520.	10.2	109
288	A New Design Paradigm for Smart Windows: Photocurable Polymers for Quasiâ€5olid Photoelectrochromic Devices with Excellent Longâ€Term Stability under Real Outdoor Operating Conditions. Advanced Functional Materials, 2016, 26, 1127-1137.	7.8	109

#	Article	IF	CITATIONS
289	Highly Efficient and Stable Perovskite Solar Cells based on a Lowâ€Cost Carbon Cloth. Advanced Energy Materials, 2016, 6, 1601116.	10.2	107
290	Passivation Mechanism Exploiting Surface Dipoles Affords High-Performance Perovskite Solar Cells. Journal of the American Chemical Society, 2020, 142, 11428-11433.	6.6	107
291	Adamantanes Enhance the Photovoltaic Performance and Operational Stability of Perovskite Solar Cells by Effective Mitigation of Interfacial Defect States. Advanced Energy Materials, 2018, 8, 1800275.	10.2	106
292	Greener, Nonhalogenated Solvent Systems for Highly Efficient Perovskite Solar Cells. Advanced Energy Materials, 2018, 8, 1800177.	10.2	106
293	A–D–A-type S,N-heteropentacene-based hole transport materials for dopant-free perovskite solar cells. Journal of Materials Chemistry A, 2015, 3, 17738-17746.	5.2	105
294	High Open-Circuit Voltage: Fabrication of Formamidinium Lead Bromide Perovskite Solar Cells Using Fluorene–Dithiophene Derivatives as Hole-Transporting Materials. ACS Energy Letters, 2016, 1, 107-112.	8.8	105
295	Proof-of-concept for facile perovskite solar cell recycling. Energy and Environmental Science, 2016, 9, 3172-3179.	15.6	105
296	Ba-induced phase segregation and band gap reduction in mixed-halide inorganic perovskite solar cells. Nature Communications, 2019, 10, 4686.	5.8	105
297	Compositional and Interface Engineering of Organic-Inorganic Lead Halide Perovskite Solar Cells. IScience, 2020, 23, 101359.	1.9	105
298	High efficient donor–acceptor ruthenium complex for dye-sensitized solar cell applications. Energy and Environmental Science, 2009, 2, 100-102.	15.6	104
299	Strong Photocurrent Amplification in Perovskite Solar Cells with a Porous TiO <sub>2</sub> Blocking Layer under Reverse Bias. Journal of Physical Chemistry Letters, 2014, 5, 3931-3936.	2.1	104
300	Intrinsic and Extrinsic Stability of Formamidinium Lead Bromide Perovskite Solar Cells Yielding High Photovoltage. Nano Letters, 2016, 16, 7155-7162.	4.5	104
301	Atomic-Level Microstructure of Efficient Formamidinium-Based Perovskite Solar Cells Stabilized by 5-Ammonium Valeric Acid Iodide Revealed by Multinuclear and Two-Dimensional Solid-State NMR. Journal of the American Chemical Society, 2019, 141, 17659-17669.	6.6	104
302	New pyrido[3,4-b]pyrazine-based sensitizers for efficient and stable dye-sensitized solar cells. Chemical Science, 2014, 5, 206-214.	3.7	102
303	Efficient stable graphene-based perovskite solar cells with high flexibility in device assembling <i>via</i> modular architecture design. Energy and Environmental Science, 2019, 12, 3585-3594.	15.6	102
304	Optical analysis of CH <sub>3</sub> NH <sub>3</sub> Sn <sub>x</sub> Pb <sub>1â^'x</sub> I <sub>3</sub> absorbers: a roadmap for perovskite-on-perovskite tandem solar cells. Journal of Materials Chemistry A, 2016, 4, 11214-11221.	5.2	101
305	Band Alignment Engineering at Cu <sub>2</sub> O/ZnO Heterointerfaces. ACS Applied Materials & Interfaces, 2016, 8, 21824-21831.	4.0	101
306	Dedoping of Lead Halide Perovskites Incorporating Monovalent Cations. ACS Nano, 2018, 12, 7301-7311.	7.3	101

#	Article	IF	CITATIONS
307	Core/Shell PbSe/PbS QDs TiO <sub>2</sub> Heterojunction Solar Cell. Advanced Functional Materials, 2013, 23, 2736-2741.	7.8	99
308	The Role of Insulating Oxides in Blocking the Charge Carrier Recombination in Dye‧ensitized Solar Cells. Advanced Functional Materials, 2014, 24, 1615-1623.	7.8	99
309	Engineering of Perovskite Materials Based on Formamidinium and Cesium Hybridization for High-Efficiency Solar Cells. Chemistry of Materials, 2019, 31, 1620-1627.	3.2	99
310	Femtosecond Dynamics of Interfacial and Intermolecular Electron Transfer at Eosin-Sensitized Metal Oxide Nanoparticles. Journal of Physical Chemistry B, 2003, 107, 3215-3224.	1.2	98
311	Synthesis of mesoporous titanium dioxide by soft template based approach: characterization and application in dye-sensitized solar cells. Energy and Environmental Science, 2010, 3, 838.	15.6	98
312	Approaching truly sustainable solar cells by the use of water and cellulose derivatives. Green Chemistry, 2017, 19, 1043-1051.	4.6	98
313	High-Performance Lead-Free Solar Cells Based on Tin-Halide Perovskite Thin Films Functionalized by a Divalent Organic Cation. ACS Energy Letters, 2020, 5, 2223-2230.	8.8	96
314	A Ga <sub>2</sub> O <sub>3</sub> underlayer as an isomorphic template for ultrathin hematite films toward efficient photoelectrochemical water splitting. Faraday Discussions, 2012, 155, 223-232.	1.6	95
315	One-step mechanochemical incorporation of an insoluble cesium additive for high performance planar heterojunction solar cells. Nano Energy, 2018, 49, 523-528.	8.2	95
316	Black phosphorus quantum dots in inorganic perovskite thin films for efficient photovoltaic application. Science Advances, 2020, 6, eaay5661.	4.7	95
317	Stable and Efficient Organic Dye-Sensitized Solar Cell Based on Ionic Liquid Electrolyte. Joule, 2018, 2, 2145-2153.	11.7	94
318	Thermochemical Stability of Hybrid Halide Perovskites. ACS Energy Letters, 2019, 4, 2859-2870.	8.8	91
319	A water-based and metal-free dye solar cell exceeding 7% efficiency using a cationic poly(3,4-ethylenedioxythiophene) derivative. Chemical Science, 2020, 11, 1485-1493.	3.7	91
320	Silica-copper catalyst interfaces enable carbon-carbon coupling towards ethylene electrosynthesis. Nature Communications, 2021, 12, 2808.	5.8	91
321	Unveiling iodine-based electrolytes chemistry in aqueous dye-sensitized solar cells. Chemical Science, 2016, 7, 4880-4890.	3.7	90
322	High performance carbon-based printed perovskite solar cells with humidity assisted thermal treatment. Journal of Materials Chemistry A, 2017, 5, 12060-12067.	5.2	90
323	A copper nickel mixed oxide hole selective layer for Au-free transparent cuprous oxide photocathodes. Energy and Environmental Science, 2017, 10, 912-918.	15.6	90
324	Solution-Processed Cu <sub>2</sub> S Photocathodes for Photoelectrochemical Water Splitting. ACS Energy Letters, 2018, 3, 760-766.	8.8	89

#	Article	IF	CITATIONS
325	Supramolecular Engineering for Formamidiniumâ€Based Layered 2D Perovskite Solar Cells: Structural Complexity and Dynamics Revealed by Solidâ€State NMR Spectroscopy. Advanced Energy Materials, 2019, 9, 1900284.	10.2	89
326	Efficient and stable noble-metal-free catalyst for acidic water oxidation. Nature Communications, 2022, 13, 2294.	5.8	89
327	Indirect tail states formation by thermal-induced polar fluctuations in halide perovskites. Nature Communications, 2019, 10, 484.	5.8	88
328	Intermediate Phase Enhances Inorganic Perovskite and Metal Oxide Interface for Efficient Photovoltaics. Joule, 2020, 4, 222-234.	11.7	88
329	A novel one-step synthesized and dopant-free hole transport material for efficient and stable perovskite solar cells. Journal of Materials Chemistry A, 2016, 4, 16330-16334.	5.2	87
330	A new efficient photosensitizer for nanocrystalline solar cells: synthesis and characterization of cis-bis(4,7-dicarboxy-1,10-phenanthroline)dithiocyanato ruthenium(II). Dalton Transactions RSC, 2000, , 2817-2822.	2.3	86
331	Polymer-based photocathodes with a solution-processable cuprous iodide anode layer and a polyethyleneimine protective coating. Energy and Environmental Science, 2016, 9, 3710-3723.	15.6	86
332	Effect of Interfacial Engineering in Solid‣tate Nanostructured Sb <sub>2</sub> S <sub>3</sub> Heterojunction Solar Cells. Advanced Energy Materials, 2013, 3, 29-33.	10.2	85
333	Impact of a Mesoporous Titania–Perovskite Interface on the Performance of Hybrid Organic–Inorganic Perovskite Solar Cells. Journal of Physical Chemistry Letters, 2016, 7, 3264-3269.	2.1	85
334	Revealing the detailed path of sequential deposition for metal halide perovskite formation. Science Advances, 2018, 4, e1701402.	4.7	85
335	Hydrothermally processed CuCrO <sub>2</sub> nanoparticles as an inorganic hole transporting material for low-cost perovskite solar cells with superior stability. Journal of Materials Chemistry A, 2018, 6, 20327-20337.	5.2	85
336	Analysing the effect of crystal size and structure in highly efficient CH <sub>3</sub> NH <sub>3</sub> PbI <sub>3</sub> perovskite solar cells by spatially resolved photo- and electroluminescence imaging. Nanoscale, 2015, 7, 19653-19662.	2.8	84
337	Tin oxide as stable protective layer for composite cuprous oxide water-splitting photocathodes. Nano Energy, 2016, 24, 10-16.	8.2	84
338	Dopantâ€Free Donor (D)–π–D–π–D Conjugated Holeâ€Transport Materials for Efficient and Stable Perovskite Solar Cells. ChemSusChem, 2016, 9, 2578-2585.	3.6	83
339	Spectroelectrochemical analysis of the mechanism of (photo)electrochemical hydrogen evolution at a catalytic interface. Nature Communications, 2017, 8, 14280.	5.8	83
340	Dopant-free star-shaped hole-transport materials for efficient and stable perovskite solar cells. Dyes and Pigments, 2017, 136, 273-277.	2.0	83
341	Lowâ€Cost and Highly Efficient Carbonâ€Based Perovskite Solar Cells Exhibiting Excellent Longâ€Term Operational and UV Stability. Small, 2019, 15, e1904746.	5.2	83
342	A deep-blue emitting charged bis-cyclometallated iridium( <scp>iii</scp> ) complex for light-emitting electrochemical cells. Journal of Materials Chemistry C, 2013, 1, 58-68.	2.7	81

#	Article	IF	CITATIONS
343	Globularity‧elected Large Molecules for a New Generation of Multication Perovskites. Advanced Materials, 2017, 29, 1702005.	11.1	81
344	Controlled synthesis of TiO <sub>2</sub> nanoparticles and nanospheres using a microwave assisted approach for their application in dye-sensitized solar cells. Journal of Materials Chemistry A, 2014, 2, 1662-1667.	5.2	80
345	A Novel Oligomer as a Hole Transporting Material for Efficient Perovskite Solar Cells. Advanced Energy Materials, 2015, 5, 1400980.	10.2	80
346	Ligand Engineering for the Efficient Dye-Sensitized Solar Cells with Ruthenium Sensitizers and Cobalt Electrolytes. Inorganic Chemistry, 2016, 55, 6653-6659.	1.9	80
347	Long term stability of air processed inkjet infiltrated carbon-based printed perovskite solar cells under intense ultra-violet light soaking. Journal of Materials Chemistry A, 2017, 5, 4797-4802.	5.2	80
348	Symmetric vs. asymmetric squaraines as photosensitisers in mesoscopic injection solar cells: a structure–property relationship study. Chemical Communications, 2012, 48, 2782.	2.2	79
349	Mechanoperovskites for Photovoltaic Applications: Preparation, Characterization, and Device Fabrication. Accounts of Chemical Research, 2019, 52, 3233-3243.	7.6	79
350	Metal Coordination Complexes as Redox Mediators in Regenerative Dye-Sensitized Solar Cells. Inorganics, 2019, 7, 30.	1.2	79
351	Mechanosynthesis of pure phase mixed-cation MA <sub>x</sub> FA <sub>1â^²x</sub> PbI <sub>3</sub> hybrid perovskites: photovoltaic performance and electrochemical properties. Sustainable Energy and Fuels, 2017, 1, 689-693.	2.5	78
352	Suppressed recombination for monolithic inorganic perovskite/silicon tandem solar cells with an approximate efficiency of 23%. EScience, 2022, 2, 339-346.	25.0	78
353	Melt-infiltration of spiro-OMeTAD and thermal instability of solid-state dye-sensitized solar cells. Physical Chemistry Chemical Physics, 2014, 16, 4864.	1.3	77
354	A universal co-solvent dilution strategy enables facile and cost-effective fabrication of perovskite photovoltaics. Nature Communications, 2022, 13, 89.	5.8	77
355	Inherent electronic trap states in TiO2 nanocrystals: effect of saturation and sintering. Energy and Environmental Science, 2013, 6, 1221.	15.6	76
356	Butyronitrile-Based Electrolyte for Dye-Sensitized Solar Cells. Journal of the American Chemical Society, 2011, 133, 13103-13109.	6.6	75
357	Avoiding Diffusion Limitations in Cobalt(III/II)â€∢i>Tris(2,2′â€Bipyridine)â€Based Dye ensitized Solar Cel by Tuning the Mesoporous TiO <sub>2</sub> Film Properties. ChemPhysChem, 2012, 13, 2976-2981.	lls 1.0	75
358	Strategic advantages of reactive polyiodide melts for scalable perovskite photovoltaics. Nature Nanotechnology, 2019, 14, 57-63.	15.6	75
359	Carbon Nanoparticles in Highâ€Performance Perovskite Solar Cells. Advanced Energy Materials, 2018, 8, 1702719.	10.2	74
360	Dual effect of humidity on cesium lead bromide: enhancement and degradation of perovskite films. Journal of Materials Chemistry A, 2019, 7, 12292-12302.	5.2	74

#	Article	IF	CITATIONS
361	Understanding the Impact of Bromide on the Photovoltaic Performance of CH <sub>3</sub> NH <sub>3</sub> PbI <sub>3</sub> Solar Cells. Advanced Materials, 2015, 27, 7221-7228.	11.1	73
362	Direct light-induced polymerization of cobalt-based redox shuttles: an ultrafast way towards stable dye-sensitized solar cells. Chemical Communications, 2015, 51, 16308-16311.	2.2	73
363	Reduction in the Interfacial Trap Density of Mechanochemically Synthesized MAPbI <sub>3</sub> . ACS Applied Materials & Interfaces, 2017, 9, 28418-28425.	4.0	73
364	High Solar Flux Concentration Water Splitting with Hematite (αâ€Fe <sub>2</sub> O <sub>3</sub> ) Photoanodes. Advanced Energy Materials, 2016, 6, 1500817.	10.2	72
365	Multimodal host–guest complexation for efficient and stable perovskite photovoltaics. Nature Communications, 2021, 12, 3383.	5.8	72
366	Ti1–graphene single-atom material for improved energy level alignment in perovskite solar cells. Nature Energy, 2021, 6, 1154-1163.	19.8	72
367	Molecular Engineering of Phthalocyanine Sensitizers for Dye-Sensitized Solar Cells. Journal of Physical Chemistry C, 2014, 118, 17166-17170.	1.5	70
368	Low-Temperature Atomic Layer Deposition of Crystalline and Photoactive Ultrathin Hematite Films for Solar Water Splitting. ACS Nano, 2015, 9, 11775-11783.	7.3	70
369	Hybrid organic–inorganic H <sub>2</sub> -evolving photocathodes: understanding the route towards high performance organic photoelectrochemical water splitting. Journal of Materials Chemistry A, 2016, 4, 2178-2187.	5.2	70
370	Gold-in-copper at low *CO coverage enables efficient electromethanation of CO2. Nature Communications, 2021, 12, 3387.	5.8	70
371	Supramolecular Modulation of Hybrid Perovskite Solar Cells via Bifunctional Halogen Bonding Revealed by Two-Dimensional <sup>19</sup> F Solid-State NMR Spectroscopy. Journal of the American Chemical Society, 2020, 142, 1645-1654.	6.6	69
372	Nanoscale interfacial engineering enables highly stable and efficient perovskite photovoltaics. Energy and Environmental Science, 2021, 14, 5552-5562.	15.6	69
373	Structure–Property Relations in Allâ€Organic Dyeâ€5ensitized Solar Cells. Advanced Functional Materials, 2013, 23, 424-429.	7.8	68
374	New Insight into the Formation of Hybrid Perovskite Nanowires via Structure Directing Adducts. Chemistry of Materials, 2017, 29, 587-594.	3.2	68
375	Photoanode/Electrolyte Interface Stability in Aqueous Dye ensitized Solar Cells. Energy Technology, 2017, 5, 300-311.	1.8	68
376	In situ growth of graphene on both sides of a Cu–Ni alloy electrode for perovskite solar cells with improved stability. Nature Energy, 2022, 7, 520-527.	19.8	68
377	Engineering of thiocyanate-free Ru(ii) sensitizers for high efficiency dye-sensitized solar cells. Chemical Science, 2013, 4, 2423.	3.7	67
378	Novel Blue Organic Dye for Dye-Sensitized Solar Cells Achieving High Efficiency in Cobalt-Based Electrolytes and by Co-Sensitization. ACS Applied Materials & Interfaces, 2016, 8, 32797-32804.	4.0	67

#	Article	IF	CITATIONS
379	Low-Cost Dopant Additive-Free Hole-Transporting Material for a Robust Perovskite Solar Cell with Efficiency Exceeding 21%. ACS Energy Letters, 2021, 6, 208-215.	8.8	67
380	Dopant Engineering for Spiroâ€OMeTAD Holeâ€Transporting Materials towards Efficient Perovskite Solar Cells. Advanced Functional Materials, 2021, 31, 2102124.	7.8	67
381	Photovoltaic and Amplified Spontaneous Emission Studies of Highâ€Quality Formamidinium Lead Bromide Perovskite Films. Advanced Functional Materials, 2016, 26, 2846-2854.	7.8	66
382	Transparent and Colorless Dye-Sensitized Solar Cells Exceeding 75% Average Visible Transmittance. Jacs Au, 2021, 1, 409-426.	3.6	66
383	Facile fabrication of tin-doped hematite photoelectrodes – effect of doping on magnetic properties and performance for light-induced water splitting. Journal of Materials Chemistry, 2012, 22, 23232.	6.7	65
384	Mesoporous TiO <sub>2</sub> Beads Offer Improved Mass Transport for Cobaltâ€Based Redox Couples Leading to High Efficiency Dye‧ensitized Solar Cells. Advanced Energy Materials, 2014, 4, 1400168.	10.2	65
385	Unravel the Impact of Anchoring Groups on the Photovoltaic Performances of Diketopyrrolopyrrole Sensitizers for Dye-Sensitized Solar Cells. ACS Sustainable Chemistry and Engineering, 2015, 3, 2389-2396.	3.2	65
386	Additiveâ€Free Transparent Triarylamineâ€Based Polymeric Holeâ€Transport Materials for Stable Perovskite Solar Cells. ChemSusChem, 2016, 9, 2567-2571.	3.6	65
387	Dye-sensitized solar cells with inkjet-printed dyes. Energy and Environmental Science, 2016, 9, 2453-2462.	15.6	65
388	Xanthanâ€Based Hydrogel for Stable and Efficient Quasiâ€Solid Truly Aqueous Dyeâ€Sensitized Solar Cell with Cobalt Mediator. Solar Rrl, 2021, 5, 2000823.	3.1	65
389	Harnessing the open-circuit voltage via a new series of Ru(ii) sensitizers bearing (iso-)quinolinyl pyrazolate ancillaries. Energy and Environmental Science, 2013, 6, 859.	15.6	64
390	Rational design of triazatruxene-based hole conductors for perovskite solar cells. RSC Advances, 2015, 5, 53426-53432.	1.7	64
391	Pulsed-current versus constant-voltage light-emitting electrochemical cells with trifluoromethyl-substituted cationic iridium(iii) complexes. Journal of Materials Chemistry C, 2013, 1, 2241.	2.7	63
392	Effect of Extended ï€-Conjugation of the Donor Structure of Organic D–Aâ^'ï€â€"A Dyes on the Photovoltaic Performance of Dye-Sensitized Solar Cells. Journal of Physical Chemistry C, 2014, 118, 16486-16493.	1.5	63
393	Electrochemical Properties of Cu(II/I)-Based Redox Mediators for Dye-Sensitized Solar Cells. Electrochimica Acta, 2017, 227, 194-202.	2.6	63
394	Evolution of an Oxygen Near-Edge X-ray Absorption Fine Structure Transition in the Upper Hubbard Band in α-Fe <sub>2</sub> O <sub>3</sub> upon Electrochemical Oxidation. Journal of Physical Chemistry C, 2011, 115, 5619-5625.	1.5	62
395	Efficient orange light-emitting electrochemical cells. Journal of Materials Chemistry, 2012, 22, 19264.	6.7	62
396	High performance dye-sensitized solar cells with inkjet printed ionic liquid electrolyte. Nano Energy, 2015, 17, 206-215.	8.2	62

#	Article	IF	CITATIONS
397	Highâ€Efficiency Perovskite Solar Cells Employing a <i>S</i> , <i>N</i> â€Heteropentaceneâ€based D–A Holeâ€Transport Material. ChemSusChem, 2016, 9, 433-438.	3.6	61
398	Guanine‧tabilized Formamidinium Lead Iodide Perovskites. Angewandte Chemie - International Edition, 2020, 59, 4691-4697.	7.2	61
399	Formamidiniumâ€Based Dionâ€Jacobson Layered Hybrid Perovskites: Structural Complexity and Optoelectronic Properties. Advanced Functional Materials, 2020, 30, 2003428.	7.8	61
400	Porphyrin Sensitizers Bearing a Pyridine-Type Anchoring Group for Dye-Sensitized Solar Cells. ACS Applied Materials & Interfaces, 2015, 7, 14975-14982.	4.0	60
401	Elucidation of Charge Recombination and Accumulation Mechanism in Mixed Perovskite Solar Cells. Journal of Physical Chemistry C, 2018, 122, 15149-15154.	1.5	59
402	Doping and phase segregation in Mn <sup>2+</sup> - and Co <sup>2+</sup> -doped lead halide perovskites from <sup>133</sup> Cs and <sup>1</sup> H NMR relaxation enhancement. Journal of Materials Chemistry A, 2019, 7, 2326-2333.	5.2	59
403	Phenanthreneâ€Fusedâ€Quinoxaline as a Key Building Block for Highly Efficient and Stable Sensitizers in Copperâ€Electrolyteâ€Based Dyeâ€Sensitized Solar Cells. Angewandte Chemie - International Edition, 2020, 59, 9324-9329.	7.2	59
404	Facile synthesis of a bulky BPTPA donor group suitable for cobalt electrolyte based dye sensitized solar cells. Journal of Materials Chemistry A, 2013, 1, 5535.	5.2	58
405	Influence of the Nature of A Cation on Dynamics of Charge Transfer Processes in Perovskite Solar Cells. Advanced Functional Materials, 2018, 28, 1706073.	7.8	58
406	A chain is as strong as its weakest link – Stability study of MAPbI3 under light and temperature. Materials Today, 2019, 29, 10-19.	8.3	58
407	Over 24% efficient MA-free CsxFA1â^'xPbX3 perovskite solar cells. Joule, 2022, 6, 1344-1356.	11.7	58
408	Poly(ethylene glycol)–[60]Fullereneâ€Based Materials for Perovskite Solar Cells with Improved Moisture Resistance and Reduced Hysteresis. ChemSusChem, 2018, 11, 1032-1039.	3.6	57
409	An ultrathin cobalt–iron oxide catalyst for water oxidation on nanostructured hematite photoanodes. Journal of Materials Chemistry A, 2019, 7, 6012-6020.	5.2	57
410	Organic Ammonium Halide Modulators as Effective Strategy for Enhanced Perovskite Photovoltaic Performance. Advanced Science, 2021, 8, 2004593.	5.6	57
411	Surface Reconstruction Engineering with Synergistic Effect of Mixedâ€Salt Passivation Treatment toward Efficient and Stable Perovskite Solar Cells. Advanced Functional Materials, 2021, 31, 2102902.	7.8	57
412	Evaluating the Critical Thickness of TiO <sub>2</sub> Layer on Insulating Mesoporous Templates for Efficient Current Collection in Dye‧ensitized Solar Cells. Advanced Functional Materials, 2013, 23, 2775-2781.	7.8	56
413	Tridentate cobalt complexes as alternative redox couples for high-efficiency dye-sensitized solar cells. Chemical Science, 2013, 4, 454-459.	3.7	56
414	Calculation of the Energy Band Diagram of a Photoelectrochemical Water Splitting Cell. Journal of Physical Chemistry C, 2014, 118, 29599-29607.	1.5	56

#	Article	IF	CITATIONS
415	Electronâ€Affinityâ€Triggered Variations on the Optical and Electrical Properties of Dye Molecules Enabling Highly Efficient Dye‧ensitized Solar Cells. Angewandte Chemie - International Edition, 2018, 57, 14125-14128.	7.2	56
416	Sequential catalysis enables enhanced C–C coupling towards multi-carbon alkenes and alcohols in carbon dioxide reduction: a study on bifunctional Cu/Au electrocatalysts. Faraday Discussions, 2019, 215, 282-296.	1.6	56
417	Preferential Orientation in Hematite Films for Solar Hydrogen Production via Water Splitting. Chemical Vapor Deposition, 2010, 16, 291-295.	1.4	55
418	Nanoscale Phase Segregation in Supramolecular π-Templating for Hybrid Perovskite Photovoltaics from NMR Crystallography. Journal of the American Chemical Society, 2021, 143, 1529-1538.	6.6	55
419	Benzotrithiopheneâ€Based Holeâ€Transporting Materials for 18.2 % Perovskite Solar Cells. Angewandte Chemie, 2016, 128, 6378-6382.	1.6	54
420	A durable SWCNT/PET polymer foil based metal free counter electrode for flexible dye-sensitized solar cells. Journal of Materials Chemistry A, 2014, 2, 19609-19615.	5.2	53
421	Suppressing recombination in perovskite solar cells via surface engineering of TiO2 ETL. Solar Energy, 2020, 197, 50-57.	2.9	53
422	Preparation of tin dioxide nanotubes via electrosynthesis in a template. Journal of Materials Chemistry, 2006, 16, 2843-2845.	6.7	52
423	Photoinduced Interfacial Electron Injection Dynamics in Dye-Sensitized Solar Cells under Photovoltaic Operating Conditions. Journal of Physical Chemistry Letters, 2012, 3, 3786-3790.	2.1	52
424	Dye-sensitized solar cells using cobalt electrolytes: the influence of porosity and pore size to achieve high-efficiency. Journal of Materials Chemistry C, 2017, 5, 2833-2843.	2.7	52
425	Seeâ€Through Dyeâ€Sensitized Solar Cells: Photonic Reflectors for Tandem and Building Integrated Photovoltaics. Advanced Materials, 2013, 25, 5734-5741.	11.1	51
426	Metalâ€Halide Perovskites for Gate Dielectrics in Fieldâ€Effect Transistors and Photodetectors Enabled by PMMA Liftâ€Off Process. Advanced Materials, 2018, 30, e1707412.	11.1	51
427	Copolymerâ€Templated Nickel Oxide for Highâ€Efficiency Mesoscopic Perovskite Solar Cells in Inverted Architecture. Advanced Functional Materials, 2021, 31, 2102237.	7.8	51
428	Light scattering enhancement from sub-micrometer cavities in the photoanode for dye-sensitized solar cells. Journal of Materials Chemistry, 2012, 22, 16201.	6.7	50
429	Dopant-Free Hole-Transporting Polymers for Efficient and Stable Perovskite Solar Cells. Macromolecules, 2019, 52, 2243-2254.	2.2	50
430	Fabrication and performance of a monolithic dye-sensitized TiO2/Cu(In,Ga)Se2 thin film tandem solar cell. Applied Physics Letters, 2009, 94, 173508.	1.5	49
431	Utilization of Direct and Diffuse Sunlight in a Dye-Sensitized Solar Cell — Silicon Photovoltaic Hybrid Concentrator System. Journal of Physical Chemistry Letters, 2011, 2, 581-585.	2.1	49
432	Organic Sensitizers with Bridged Triphenylamine Donor Units for Efficient Dye‣ensitized Solar Cells. Advanced Energy Materials, 2013, 3, 200-205.	10.2	49

#	Article	IF	CITATIONS
433	Effect of Coordination Sphere Geometry of Copper Redox Mediators on Regeneration and Recombination Behavior in Dye-Sensitized Solar Cell Applications. ACS Applied Energy Materials, 2018, 1, 4950-4962.	2.5	49
434	A combined molecular dynamics and experimental study of two-step process enabling low-temperature formation of phase-pure α-FAPbI <sub>3</sub> . Science Advances, 2021, 7, .	4.7	49
435	Themed issue: nanomaterials for energy conversion and storage. Journal of Materials Chemistry, 2012, 22, 24190.	6.7	48
436	Room temperature formation of organic–inorganic lead halide perovskites: design of nanostructured and highly reactive intermediates. Journal of Materials Chemistry A, 2017, 5, 3599-3608.	5.2	48
437	Layered Hybrid Formamidinium Lead Iodide Perovskites: Challenges and Opportunities. Accounts of Chemical Research, 2021, 54, 2729-2740.	7.6	48
438	Synthesis, characterization and ab initio investigation of a panchromatic ullazine–porphyrin photosensitizer for dye-sensitized solar cells. Journal of Materials Chemistry A, 2016, 4, 2332-2339.	5.2	47
439	Chemically tailored molecular surface modifiers for efficient and stable perovskite photovoltaics. SmartMat, 2021, 2, 33-37.	6.4	47
440	Morphology Engineering: A Route to Highly Reproducible and High Efficiency Perovskite Solar Cells. ChemSusChem, 2017, 10, 1624-1630.	3.6	46
441	Slow CH <sub>3</sub> NH <sub>3</sub> <sup>+</sup> Diffusion in CH <sub>3</sub> NH <sub>3</sub> PbI <sub>3</sub> under Light Measured by Solid-State NMR and Tracer Diffusion. Journal of Physical Chemistry C, 2018, 122, 21803-21806.	1.5	46
442	Combined Precursor Engineering and Grain Anchoring Leading to MAâ€Free, Phaseâ€Pure, and Stable αâ€Formamidinium Lead Iodide Perovskites for Efficient Solar Cells. Angewandte Chemie - International Edition, 2021, 60, 27299-27306.	7.2	46
443	Diketopyrrolopyrrole-based sensitizers for dye-sensitized solar cell applications: anchor engineering. Journal of Materials Chemistry A, 2013, 1, 13978.	5.2	45
444	Molecular Design of Efficient Organic D–A––A Dye Featuring Triphenylamine as Donor Fragment for Application in Dye‣ensitized Solar Cells. ChemSusChem, 2018, 11, 494-502.	3.6	45
445	Reduced Graphene Oxide as a Stabilizing Agent in Perovskite Solar Cells. Advanced Materials Interfaces, 2018, 5, 1800416.	1.9	45
446	Atomistic Mechanism of the Nucleation of Methylammonium Lead Iodide Perovskite from Solution. Chemistry of Materials, 2020, 32, 529-536.	3.2	45
447	Unravelling the Behavior of Dion–Jacobson Layered Hybrid Perovskites in Humid Environments. ACS Energy Letters, 2021, 6, 337-344.	8.8	44
448	Novel Nanoâ€Structured Silicaâ€Based Electrolytes Containing Quaternary Ammonium Iodide Moieties. Advanced Functional Materials, 2007, 17, 3200-3206.	7.8	43
449	Unsymmetrical squaraine dimer with an extended π-electron framework: An approach in harvesting near infra-red photons for energy conversion. Dyes and Pigments, 2010, 87, 30-38.	2.0	43
450	Stabilizing organic photocathodes by low-temperature atomic layer deposition of TiO <sub>2</sub> . Sustainable Energy and Fuels, 2017, 1, 1915-1920.	2.5	43

#	Article	IF	CITATIONS
451	Effect of Cs-Incorporated NiO <sub><i>x</i></sub> on the Performance of Perovskite Solar Cells. ACS Omega, 2017, 2, 9074-9079.	1.6	43
452	Structural and photocatalytic properties of perovskite-type (La,Ca)Ti(O,N)3 prepared from A-site deficient precursors. Journal of Materials Chemistry, 2012, 22, 17906.	6.7	42
453	Unraveling the Impact of Rubidium Incorporation on the Transport-Recombination Mechanisms in Highly Efficient Perovskite Solar Cells by Small-Perturbation Techniques. Journal of Physical Chemistry C, 2017, 121, 24903-24908.	1.5	42
454	Anisotropic photocatalytic properties of hematite. Aquatic Sciences, 2009, 71, 151-159.	0.6	41
455	Panchromatic symmetrical squaraines: a step forward in the molecular engineering of low cost blue-greenish sensitizers for dye-sensitized solar cells. Physical Chemistry Chemical Physics, 2014, 16, 24173-24177.	1.3	41
456	Orientationâ€Engineered Smallâ€Molecule Semiconductors as Dopantâ€Free Hole Transporting Materials for Efficient and Stable Perovskite Solar Cells. Advanced Functional Materials, 2021, 31, 2011270.	7.8	41
457	Donorâ€i€â€Acceptors Containing the 10â€(1,3â€Dithiolâ€2â€ylidene)anthracene Unit for Dyeâ€5ensitized Sola Chemistry - A European Journal, 2012, 18, 11621-11629.	r Cells. 1.7	40
458	Formation of an electron hole doped film in the α-Fe <sub>2</sub> O <sub>3</sub> photoanode upon electrochemical oxidation. Physical Chemistry Chemical Physics, 2013, 15, 1443-1451.	1.3	40
459	Hill climbing hysteresis of perovskiteâ€based solar cells: a maximum power point tracking investigation. Progress in Photovoltaics: Research and Applications, 2017, 25, 942-950.	4.4	40
460	Enhancement of Electrochemical Activity of LiFePO <sub>4</sub> (olivine) by Amphiphilic Ru-bipyridine Complex Anchored to a Carbon Nanotube. Chemistry of Materials, 2007, 19, 4716-4721.	3.2	39
461	Photoanode Based on (001)-Oriented Anatase Nanoplatelets for Organic–Inorganic Lead Iodide Perovskite Solar Cell. Chemistry of Materials, 2014, 26, 4675-4678.	3.2	39
462	CNT-based bifacial perovskite solar cells toward highly efficient 4-terminal tandem photovoltaics. Energy and Environmental Science, 2022, 15, 1536-1544.	15.6	39
463	Computational Characterization of the Dependence of Halide Perovskite Effective Masses on Chemical Composition and Structure. Journal of Physical Chemistry C, 2017, 121, 23886-23895.	1.5	38
464	Alternative bases to 4-tert-butylpyridine for dye-sensitized solar cells employing copper redox mediator. Electrochimica Acta, 2018, 265, 194-201.	2.6	38
465	Application of Cu(ii) and Zn(ii) coproporphyrins as sensitizers for thin film dye sensitized solar cells. Energy and Environmental Science, 2010, 3, 956.	15.6	37
466	High Open-Circuit Voltages: Evidence for a Sensitizer-Induced TiO2 Conduction Band Shift in Ru(II)-Dye Sensitized Solar Cells. Chemistry of Materials, 2013, 25, 4497-4502.	3.2	37
467	Passivation of ZnO Nanowire Guests and 3D Inverse Opal Host Photoanodes for Dyeâ€Sensitized Solar Cells. Advanced Energy Materials, 2014, 4, 1400217.	10.2	37
468	Charge carrier chemistry in methylammonium lead iodide. Solid State Ionics, 2018, 321, 69-74.	1.3	37

#	Article	IF	CITATIONS
469	Perowskitâ€Solarzellen: atomare Ebene, Schichtqualitäund Leistungsfäigkeit der Zellen. Angewandte Chemie, 2018, 130, 2582-2598.	1.6	37
470	Siteâ€selective Synthesis of βâ€[70]PCBMâ€like Fullerenes: Efficient Application in Perovskite Solar Cells. Chemistry - A European Journal, 2019, 25, 3224-3228.	1.7	37
471	Growth Engineering of CH <sub>3</sub> NH <sub>3</sub> PbI <sub>3</sub> Structures for Highâ€Efficiency Solar Cells. Advanced Energy Materials, 2016, 6, 1501358.	10.2	36
472	An Oxa[5]helicene-Based Racemic Semiconducting Glassy Film for Photothermally Stable Perovskite Solar Cells. IScience, 2019, 15, 234-242.	1.9	36
473	Minimizing the Trade-Off between Photocurrent and Photovoltage in Triple-Cation Mixed-Halide Perovskite Solar Cells. Journal of Physical Chemistry Letters, 2020, 11, 10188-10195.	2.1	36
474	Solidâ€ <del>S</del> tate Dyeâ€Sensitized Solar Cells Using a Novel Class of Ullazine Dyes as Sensitizers. Advanced Energy Materials, 2013, 3, 496-504.	10.2	35
475	Mesoscopic photosystems for solar light harvesting and conversion: facile and reversible transformation of metal-halide perovskites. Faraday Discussions, 2014, 176, 251-269.	1.6	35
476	Toward Higher Photovoltage: Effect of Blocking Layer on Cobalt Bipyridine Pyrazole Complexes as Redox Shuttle for Dye-Sensitized Solar Cells. Journal of Physical Chemistry C, 2014, 118, 16799-16805.	1.5	35
477	PbZrTiO <sub>3</sub> ferroelectric oxide as an electron extraction material for stable halide perovskite solar cells. Sustainable Energy and Fuels, 2019, 3, 382-389.	2.5	35
478	Ruddlesden–Popper Phases of Methylammonium-Based Two-Dimensional Perovskites with 5-Ammonium Valeric Acid AVA <sub>2</sub> MA <sub><i>n</i>–1</sub> Pb <sub><i>n</i></sub> I <sub>3<i>n</i>+1</sub> with <i>n</i> = 1, 2, and 3. Journal of Physical Chemistry Letters, 2019, 10, 3543-3549.	2.1	35
479	Intrinsic and interfacial kinetics of perovskite solar cells under photo and bias-induced degradation and recovery. Journal of Materials Chemistry C, 2017, 5, 7799-7805.	2.7	34
480	Impact of the Synthesis Route on the Water Oxidation Kinetics of Hematite Photoanodes. Journal of Physical Chemistry Letters, 2020, 11, 7285-7290.	2.1	34
481	Electron-Selective Layers for Dye-Sensitized Solar Cells Based on TiO <sub>2</sub> and SnO <sub>2</sub> . Journal of Physical Chemistry C, 2020, 124, 6512-6521.	1.5	34
482	Atomic Layer Deposition of ZnO on CuO Enables Selective and Efficient Electroreduction of Carbon Dioxide to Liquid Fuels. Angewandte Chemie, 2019, 131, 15178-15182.	1.6	33
483	Covalent Organic Framework Nanoplates Enable Solution-Processed Crystalline Nanofilms for Photoelectrochemical Hydrogen Evolution. Journal of the American Chemical Society, 2022, 144, 10291-10300.	6.6	33
484	Formation of Highâ€Performance Multiâ€Cation Halide Perovskites Photovoltaics by δâ€CsPbl <sub>3</sub> /δâ€RbPbl <sub>3</sub> Seedâ€Assisted Heterogeneous Nucleation. Advanced Energy Materials, 2021, 11, 2003785.	10.2	32
485	A New 1,3,4â€Oxadiazoleâ€Based Holeâ€Transport Material for Efficient CH <sub>3</sub> NH <sub>3</sub> PbBr <sub>3</sub> Perovskite Solar Cells. ChemSusChem, 2016, 9, 657-661.	3.6	31
486	Donor–Acceptor-Type <i>S</i> , <i>N</i> -Heteroacene-Based Hole-Transporting Materials for Efficient Perovskite Solar Cells. ACS Applied Materials & Interfaces, 2017, 9, 44423-44428.	4.0	31

#	Article	IF	CITATIONS
487	Molecular Engineering of Simple Metalâ€Free Organic Dyes Derived from Triphenylamine for Dyeâ€Sensitized Solar Cell Applications. ChemSusChem, 2020, 13, 212-220.	3.6	31
488	Asymmetric Cathodoluminescence Emission in CH <sub>3</sub> NH <sub>3</sub> Pbl <sub>3–<i>x</i></sub> Br <sub><i>x</i></sub> Perovskite Single Crystals. ACS Photonics, 2016, 3, 947-952.	3.2	30
489	Blue Photosensitizer with Copper(II/I) Redox Mediator for Efficient and Stable Dyeâ€Sensitized Solar Cells. Advanced Functional Materials, 2020, 30, 2004804.	7.8	30
490	Molecular Origin and Electrochemical Influence of Capacitive Surface States on Iron Oxide Photoanodes. Journal of Physical Chemistry C, 2016, 120, 3250-3258.	1.5	29
491	All Solution-Processed, Hybrid Organic–Inorganic Photocathode for Hydrogen Evolution. ACS Omega, 2017, 2, 3424-3431.	1.6	29
492	The role of the hole-transport layer in perovskite solar cells - reducing recombination and increasing absorption. , 2014, , .		28
493	High Absorption Coefficient Cyclopentadithiophene Donor-Free Dyes for Liquid and Solid-State Dye-Sensitized Solar Cells. Journal of Physical Chemistry C, 2016, 120, 15027-15034.	1.5	28
494	Kinetics of Ion-Exchange Reactions in Hybrid Organic–Inorganic Perovskite Thin Films Studied by In Situ Real-Time X-ray Scattering. Journal of Physical Chemistry Letters, 2018, 9, 6750-6754.	2.1	28
495	Interfacial and bulk properties of hole transporting materials in perovskite solar cells: spiro-MeTAD <i>versus</i> spiro-OMeTAD. Journal of Materials Chemistry A, 2020, 8, 8527-8539.	5.2	28
496	Benzylammoniumâ€Mediated Formamidinium Lead Iodide Perovskite Phase Stabilization for Photovoltaics. Advanced Functional Materials, 2021, 31, 2101163.	7.8	28
497	Crystalâ€6izeâ€Induced Band Gap Tuning in Perovskite Films. Angewandte Chemie - International Edition, 2021, 60, 21368-21376.	7.2	28
498	Methylammonium Triiodide for Defect Engineering of High-Efficiency Perovskite Solar Cells. ACS Energy Letters, 2021, 6, 3650-3660.	8.8	28
499	Thiocyanateâ€Free Ru(II) Sensitizers with a 4,4′â€Dicarboxyvinylâ€2,2′â€bipyridine Anchor for Dyeâ€Sensit Solar Cells. Advanced Functional Materials, 2013, 23, 2285-2294.	ized 7.8	27
500	Kinetics of the Regeneration by Iodide of Dye Sensitizers Adsorbed on Mesoporous Titania. Journal of Physical Chemistry C, 2014, 118, 17108-17115.	1.5	26
501	Function Follows Form: Correlation between the Growth and Local Emission of Perovskite Structures and the Performance of Solar Cells. Advanced Functional Materials, 2017, 27, 1701433.	7.8	26
502	Investigation on the Interface Modification of TiO <sub>2</sub> Surfaces by Functional Coâ€Adsorbents for Highâ€Efficiency Dyeâ€Sensitized Solar Cells. ChemPhysChem, 2017, 18, 2724-2731.	1.0	26
503	Electronâ€Affinityâ€Triggered Variations on the Optical and Electrical Properties of Dye Molecules Enabling Highly Efficient Dyeâ€Sensitized Solar Cells. Angewandte Chemie, 2018, 130, 14321-14324.	1.6	26
504	SnS Quantum Dots as Hole Transporter of Perovskite Solar Cells. ACS Applied Energy Materials, 2019, 2, 3822-3829.	2.5	26

#	Article	IF	CITATIONS
505	Cyclopentadithiophene-Based Hole-Transporting Material for Highly Stable Perovskite Solar Cells with Stabilized Efficiencies Approaching 21%. ACS Applied Energy Materials, 2020, 3, 7456-7463.	2.5	26
506	Spectroelectrochemical and Chemical Evidence of Surface Passivation at Zinc Ferrite (ZnFe <sub>2</sub> O <sub>4</sub> ) Photoanodes for Solar Water Oxidation. Advanced Functional Materials, 2021, 31, 2010081.	7.8	26
507	The electronic, chemical and electrocatalytic processes and intermediates on iron oxide surfaces during photoelectrochemical water splitting. Catalysis Today, 2016, 260, 72-81.	2.2	25
508	Charge Accumulation, Recombination, and Their Associated Time Scale in Efficient (GUA) <i><sub>x</sub></i> (MA) <sub>1–<i>x</i></sub> PbI <sub>3</sub> -Based Perovskite Solar Cells. ACS Omega, 2019, 4, 16840-16846.	1.6	25
509	Photovoltaic performance of injection solar cells and other applications of nanocrystalline oxide layers. Journal of Chemical Sciences, 1997, 109, 447-469.	0.7	24
510	ORGANOMETAL HALIDE PEROVSKITE PHOTOVOLTAICS: A DIAMOND IN THE ROUGH. Nano, 2014, 09, 1440002.	0.5	24
511	Thiadiazolo[3,4-c]pyridine Acceptor Based Blue Sensitizers for High Efficiency Dye-Sensitized Solar Cells. Journal of Physical Chemistry C, 2014, 118, 17090-17099.	1.5	24
512	Nanocolumnar 1-dimensional TiO <sub>2</sub> photoanodes deposited by PVD-OAD for perovskite solar cell fabrication. Journal of Materials Chemistry A, 2015, 3, 13291-13298.	5.2	24
513	Nondestructive Probing of Perovskite Silicon Tandem Solar Cells Using Multiwavelength Photoluminescence Mapping. IEEE Journal of Photovoltaics, 2017, 7, 1081-1086.	1.5	24
514	Influence of Ionic Liquid Electrolytes on the Photovoltaic Performance of Dyeâ€&ensitized Solar Cells. Energy Technology, 2017, 5, 321-326.	1.8	24
515	Interfacial Kinetics of Efficient Perovskite Solar Cells. Crystals, 2017, 7, 252.	1.0	24
516	Effect of Rubidium for Thermal Stability of Triple-cation Perovskite Solar Cells. Chemistry Letters, 2018, 47, 814-816.	0.7	24
517	Insights about the Absence of Rb Cation from the 3D Perovskite Lattice: Effect on the Structural, Morphological, and Photophysical Properties and Photovoltaic Performance. Small, 2018, 14, e1802033.	5.2	24
518	Liquid State and Zombie Dye Sensitized Solar Cells with Copper Bipyridine Complexes Functionalized with Alkoxy Groups. Journal of Physical Chemistry C, 2020, 124, 7071-7081.	1.5	24
519	A Blue Photosensitizer Realizing Efficient and Stable Green Solar Cells via Color Tuning by the Electrolyte. Advanced Materials, 2020, 32, 2000193.	11.1	24
520	Atomistic Origins of the Limited Phase Stability of Cs <sup>+</sup> -Rich FA <sub><i>x</i></sub> Cs <sub>(1–<i>x</i>)</sub> Pbl <sub>3</sub> Mixtures. Chemistry of Materials, 2020, 32, 2605-2614.	3.2	24
521	Cyclopentadieneâ€Based Holeâ€Transport Material for Costâ€Reduced Stabilized Perovskite Solar Cells with Power Conversion Efficiencies Over 23%. Advanced Energy Materials, 2021, 11, 2003953.	10.2	24
522	Acetylene-bridged dyes with high open circuit potential for dye-sensitized solar cells. RSC Advances, 2014. 4. 35251.	1.7	23

#	Article	IF	CITATIONS
523	Electronic tuning effects via π-linkers in tetrathiafulvalene-based dyes. New Journal of Chemistry, 2014, 38, 3269.	1.4	23
524	The Role of Alkyl Chain Length and Halide Counter Ion in Layered Dionâ^'Jacobson Perovskites with Aromatic Spacers. Journal of Physical Chemistry Letters, 2021, 12, 10325-10332.	2.1	23
525	Clickâ€Functionalized Ru(II) Complexes for Dyeâ€Sensitized Solar Cells. Advanced Energy Materials, 2012, 2, 1004-1012.	10.2	22
526	Ultrafast charge separation dynamics in opaque, operational dye-sensitized solar cells revealed by femtosecond diffuse reflectance spectroscopy. Scientific Reports, 2016, 6, 24465.	1.6	22
527	Perovskite Solar Cells Yielding Reproducible Photovoltage of 1.20 V. Research, 2019, 2019, 8474698.	2.8	22
528	Efficient Blueâ€Colored Solidâ€State Dyeâ€Sensitized Solar Cells: Enhanced Charge Collection by Using an in Situ Photoelectrochemically Generated Conducting Polymer Hole Conductor. ChemPhysChem, 2016, 17, 1441-1445.	1.0	21
529	Molecularly Engineered Ru(II) Sensitizers Compatible with Cobalt(II/III) Redox Mediators for Dye-Sensitized Solar Cells. Inorganic Chemistry, 2016, 55, 7388-7395.	1.9	21
530	Influence of Alkoxy Chain Length on the Properties of Twoâ€Dimensionally Expanded Azuleneâ€Coreâ€Based Holeâ€Transporting Materials for Efficient Perovskite Solar Cells. Chemistry - A European Journal, 2019, 25, 6741-6752.	1.7	21
531	A <i>peri</i> â€Xanthenoxanthene Centered Columnarâ€Stacking Organic Semiconductor for Efficient, Photothermally Stable Perovskite Solar Cells. Chemistry - A European Journal, 2019, 25, 945-948.	1.7	21
532	Water Stable Haloplumbate Modulation for Efficient and Stable Hybrid Perovskite Photovoltaics. Advanced Energy Materials, 2021, 11, 2101082.	10.2	21
533	New Insights into the Interface of Electrochemical Flow Cells for Carbon Dioxide Reduction to Ethylene. Journal of Physical Chemistry Letters, 2021, 12, 7583-7589.	2.1	21
534	Efficient and Stable Large Bandgap MAPbBr <sub>3</sub> Perovskite Solar Cell Attaining an Open Circuit Voltage of 1.65 V. ACS Energy Letters, 2022, 7, 1112-1119.	8.8	21
535	Monovalent Cation Doping of CH <sub>3</sub> NH <sub>3</sub> PbI <sub>3</sub> for Efficient Perovskite Solar Cells. Journal of Visualized Experiments, 2017, , .	0.2	20
536	Electrochemical Characterization of CuSCN Hole-Extracting Thin Films for Perovskite Photovoltaics. ACS Applied Energy Materials, 2019, 2, 4264-4273.	2.5	20
537	A hybrid bulk-heterojunction photoanode for direct solar-to-chemical conversion. Energy and Environmental Science, 2021, 14, 3141-3151.	15.6	20
538	Iron Resonant Photoemission Spectroscopy on Anodized Hematite Points to Electron Hole Doping during Anodization. ChemPhysChem, 2012, 13, 2937-2944.	1.0	19
539	Effect of Peripheral Substitution on the Performance of Subphthalocyanines in DSSCs. Chemistry - an Asian Journal, 2016, 11, 1223-1231.	1.7	19
540	Light management: porous 1-dimensional nanocolumnar structures as effective photonic crystals for perovskite solar cells. Journal of Materials Chemistry A, 2016, 4, 4962-4970.	5.2	19

Michael Grã

#	Article	IF	CITATIONS
541	Elucidation of photovoltage origin and charge transport in Cu <sub>2</sub> 0 heterojunctions for solar energy conversion. Sustainable Energy and Fuels, 2019, 3, 2633-2641.	2.5	19
542	Multifunctional Molecular Modulation for Efficient and Stable Hybrid Perovskite Solar Cells. Chimia, 2019, 73, 317.	0.3	19
543	Halide Versus Nonhalide Salts: The Effects of Guanidinium Salts on the Structural, Morphological, and Photovoltaic Performances of Perovskite Solar Cells. Solar Rrl, 2020, 4, 1900234.	3.1	19
544	Reversible Pressureâ€Dependent Mechanochromism of Dion–Jacobson and Ruddlesden–Popper Layered Hybrid Perovskites. Advanced Materials, 2022, 34, e2108720.	11.1	19
545	Between photocatalysis and photosynthesis: Synchrotron spectroscopy methods on molecules and materials for solar hydrogen generation. Journal of Electron Spectroscopy and Related Phenomena, 2013, 190, 93-105.	0.8	18
546	Nanocomposite Semiâ€Solid Redox Ionic Liquid Electrolytes with Enhanced Chargeâ€Transport Capabilities for Dyeâ€Sensitized Solar Cells. ChemSusChem, 2015, 8, 2560-2568.	3.6	18
547	Enhancing the Stability of Porphyrin Dye‣ensitized Solar Cells by Manipulation of Electrolyte Additives. ChemSusChem, 2015, 8, 255-259.	3.6	18
548	The Nature of Ion Conduction in Methylammonium Lead Iodide: A Multimethod Approach. Angewandte Chemie, 2017, 129, 7863-7867.	1.6	18
549	Analysis of Optical Losses in a Photoelectrochemical Cell: A Tool for Precise Absorptance Estimation. Advanced Functional Materials, 2018, 28, 1702768.	7.8	18
550	Hybrid 2D [Pb(CH <sub>3</sub> NH <sub>2</sub> )I <sub>2</sub> ] <sub><i>n</i></sub> Coordination Polymer Precursor for Scalable Perovskite Deposition. ACS Energy Letters, 2020, 5, 2305-2312.	8.8	18
551	Structural and Compositional Investigations on the Stability of Cuprous Oxide Nanowire Photocathodes for Photoelectrochemical Water Splitting. ACS Applied Materials & Interfaces, 2021, 13, 55080-55091.	4.0	18
552	Transparency and Morphology Control of Cu <sub>2</sub> O Photocathodes via an <i>in Situ</i> Electroconversion. ACS Energy Letters, 2022, 7, 1618-1625.	8.8	18
553	Investigation of Interfacial Charge Separation at PbS QDs/(001) TiO <sub>2</sub> Nanosheets Heterojunction Solar Cell. Particle and Particle Systems Characterization, 2015, 32, 483-488.	1.2	17
554	An Unsymmetrical, Push–Pull Porphyrazine for Dye‧ensitized Solar Cells. ChemPhotoChem, 2017, 1, 164-166.	1.5	17
555	Planar Perovskite Solar Cells with High Open ircuit Voltage Containing a Supramolecular Iron Complex as Hole Transport Material Dopant. ChemPhysChem, 2018, 19, 1363-1370.	1.0	17
556	Stabilization of Highly Efficient and Stable Phaseâ€Pure FAPbI <sub>3</sub> Perovskite Solar Cells by Molecularly Tailored 2Dâ€Overlayers. Angewandte Chemie, 2020, 132, 15818-15824.	1.6	17
557	Phenanthreneâ€Fusedâ€Quinoxaline as a Key Building Block for Highly Efficient and Stable Sensitizers in Copperâ€Electrolyteâ€Based Dyeâ€Sensitized Solar Cells. Angewandte Chemie, 2020, 132, 9410-9415.	1.6	17
558	Bis(pyrazol-1-yl)methane as Non-Chromophoric Ancillary Ligand for Charged Bis-Cyclometalated Iridium(III) Complexes. European Journal of Inorganic Chemistry, 2012, 2012, 3209-3215.	1.0	16

#	Article	IF	CITATIONS
559	Electrical Properties of <scp><scp>Nb</scp></scp> &€; <scp>Ca</scp> â€; and <scp><scp>Y</scp></scp> â€Substituted Nanocrystalline Anatase <scp>TiO</scp> 2 Prepared by Hydrothermal Synthesis. Journal of the American Ceramic Society, 2012, 95, 3192-3196.	1.9	16
560	Diffusion and adsorption of dye molecules in mesoporous TiO2 photoelectrodes studied by indirect nanoplasmonic sensing. Energy and Environmental Science, 2013, 6, 3627.	15.6	16
561	Microâ€Electrode with Fast Mass Transport for Enhancing Selectivity of Carbonaceous Products in Electrochemical CO <sub>2</sub> Reduction. Advanced Functional Materials, 2021, 31, 2103966.	7.8	16
562	Xanthanâ€Based Hydrogel for Stable and Efficient Quasiâ€Solid Truly Aqueous Dyeâ€Sensitized Solar Cell with Cobalt Mediator. Solar Rrl, 2021, 5, 2170074.	3.1	16
563	Naphthalenediimide/Formamidinium-Based Low-Dimensional Perovskites. Chemistry of Materials, 2021, 33, 6412-6420.	3.2	16
564	Adapting Ruthenium Sensitizers to Cobalt Electrolyte Systems. Journal of Physical Chemistry Letters, 2014, 5, 501-505.	2.1	15
565	Perovskite Solar Cells Yielding Reproducible Photovoltage of 1.20 V. Research, 2019, 2019, 1-9.	2.8	15
566	Benzo[1,2-b:4,5-b′]difuran-based sensitizers for dye-sensitized solar cells. RSC Advances, 2013, 3, 19798.	1.7	14
567	Decoupling light absorption and charge transport properties in near IR-sensitized Fe2O3 regenerative cells. Energy and Environmental Science, 2013, 6, 3280.	15.6	14
568	Anthanthrene dye-sensitized solar cells: influence of the number of anchoring groups and substitution motif. RSC Advances, 2015, 5, 98643-98652.	1.7	14
569	Pyridyl―and Picolinic Acid Substituted Zinc(II) Phthalocyanines for Dyeâ€Sensitized Solar Cells. ChemPlusChem, 2017, 82, 1057-1061.	1.3	14
570	Unravelling the structural complexity and photophysical properties of adamantyl-based layered hybrid perovskites. Journal of Materials Chemistry A, 2020, 8, 17732-17740.	5.2	14
571	Photo Deâ€Mixing in Dionâ€Jacobson 2D Mixed Halide Perovskites. Advanced Energy Materials, 2022, 12, .	10.2	14
572	Molecular Wiring of Olivine LiFePO <sub>4</sub> by Ruthenium(II)-Bipyridine Complexes and by Their Assemblies with Single-Walled Carbon Nanotubes. Journal of Physical Chemistry C, 2008, 112, 8708-8714.	1.5	13
573	Toward an alternative approach for the preparation of low-temperature titanium dioxide blocking underlayers for perovskite solar cells. Journal of Materials Chemistry A, 2019, 7, 10729-10738.	5.2	13
574	Quantifying Stabilized Phase Purity in Formamidinium-Based Multiple-Cation Hybrid Perovskites. Chemistry of Materials, 2021, 33, 2769-2776.	3.2	13
575	Function and Electronic Structure of the SnO2 Buffer Layer between the α-Fe2O3 Water Oxidation Photoelectrode and the Transparent Conducting Oxide Current Collector. Journal of Physical Chemistry C, 2021, 125, 9158-9168.	1.5	13
576	Revisiting the Impact of Morphology and Oxidation State of Cu on CO <sub>2</sub> Reduction Using Electrochemical Flow Cell. Journal of Physical Chemistry Letters, 2022, 13, 345-351.	2.1	13

#	Article	IF	CITATIONS
577	Interfacial engineering from material to solvent: A mechanistic understanding on stabilizing <mml:math <br="" xmlns:mml="http://www.w3.org/1998/Math/MathML">altimg="si0001.svg"&gt;<mml:mi>α</mml:mi></mml:math> -formamidinium lead triiodide perovskite photovoltaics. Nano Energy, 2022, 94, 106924.	8.2	13
578	Transition Metal Complexes as Sensitizers for Efficient Mesoscopic Solar Cells. Bulletin of Japan Society of Coordination Chemistry, 2008, 51, 3-12.	0.1	12
579	A hybrid electron donor comprising cyclopentadithiophene and dithiafulvenyl for dye-sensitized solar cells. Beilstein Journal of Organic Chemistry, 2015, 11, 1052-1059.	1.3	12
580	In-situ observation of moisture-induced degradation of perovskite solar cells using laser-beam induced current. , 2016, , .		12
581	<i>p</i> -Phenylene-bridged zinc phthalocyanine-dimer as hole-transporting material in perovskite solar cells. Journal of Porphyrins and Phthalocyanines, 2019, 23, 546-553.	0.4	12
582	Perovskite Solar Cells Based on Oligotriarylamine Hexaarylbenzene as Hole-Transporting Materials. Organic Letters, 2019, 21, 3261-3264.	2.4	12
583	Molecular Origin of the Asymmetric Photoluminescence Spectra of CsPbBr <sub>3</sub> at Low Temperature. Journal of Physical Chemistry Letters, 2021, 12, 2699-2704.	2.1	12
584	Solar Water Splitting Using Earthâ€Abundant Electrocatalysts Driven by Highâ€Efficiency Perovskite Solar Cells. ChemSusChem, 2022, 15, .	3.6	12
585	Kinetics and energeticsÂof metal halide perovskite conversion reactions at the nanoscale. Communications Materials, 2022, 3, .	2.9	12
586	A new family of substituted triethoxysilyl iodides as organic iodide sources for dye-sensitised solar cells. Journal of Materials Chemistry, 2010, 20, 3694.	6.7	11
587	Role of the Bulky Aryloxy Group at the Nonâ€Peripheral Position of Phthalocyanines for Dye Sensitized Solar Cells. ChemPlusChem, 2017, 82, 132-135.	1.3	11
588	How free exciton–exciton annihilation lets bound exciton emission dominate the photoluminescence of 2D-perovskites under high-fluence pulsed excitation at cryogenic temperatures. Journal of Applied Physics, 2021, 129, .	1.1	11
589	Methylamine Gas Treatment Affords Improving Semitransparency, Efficiency, and Stability of CH <sub>3</sub> NH <sub>3</sub> PbBr <sub>3</sub> â€Based Perovskite Solar Cells. Solar Rrl, 2021, 5, 2100277.	3.1	11
590	Identifying Reactive Sites and Surface Traps in Chalcopyrite Photocathodes. Angewandte Chemie - International Edition, 2021, 60, 23651-23655.	7.2	11
591	Combined precursor engineering and grain anchoring leading to MAâ€free, phaseâ€pure and stable αâ€formamidinium lead iodide perovskites for efficient solar cells. Angewandte Chemie, 0, , .	1.6	11
592	Nanostructures: A Smooth CH <sub>3</sub> NH <sub>3</sub> PbI <sub>3</sub> Film via a New Approach for Forming the PbI <sub>2</sub> Nanostructure Together with Strategically High CH <sub>3</sub> NH <sub>3</sub> I Concentration for High Efficient Planarâ€Heterojunction Solar Cells (Adv. Energy Mater. 23/2015). Advanced Energy Materials, 2015, 5, .	10.2	10
593	Synthesis of Amphiphilic Ru <sup>II</sup> Heteroleptic Complexes Based on Benzo[1,2â€ <i>b</i> :4,5â€ <i>b</i> à€²]dithiophene: Relevance of the Halfâ€Sandwich Complex Intermediate and Solvent Compatibility. Chemistry - A European Journal, 2015, 21, 16252-16265.	1.7	10
594	High Open Circuit Voltage for Perovskite Solar Cells with S,Siâ€Heteropentaceneâ€Based Hole Conductors. European Journal of Inorganic Chemistry, 2018, 2018, 4573-4578.	1.0	10

#	Article	IF	CITATIONS
595	Crystalâ€6izeâ€Induced Band Gap Tuning in Perovskite Films. Angewandte Chemie, 2021, 133, 21538-21546.	1.6	10
596	Multiâ€Length Scale Structure of 2D/3D Dion–Jacobson Hybrid Perovskites Based on an Aromatic Diammonium Spacer. Small, 2022, 18, e2104287.	5.2	10
597	Electrodeposition of porous CuSCN layers as hole-conducting material for perovskite solar cells. Mendeleev Communications, 2018, 28, 378-380.	0.6	9
598	Scaling effects during friction stir welding of aluminum alloys with reduced tool aspect ratios. Welding in the World, Le Soudage Dans Le Monde, 2019, 63, 337-347.	1.3	9
599	Multistep Photoluminescence Decay Reveals Dissociation of Geminate Charge Pairs in Organolead Trihalide Perovskites. Advanced Energy Materials, 2017, 7, 1700405.	10.2	8
600	A tandem redox system with a cobalt complex and 2-azaadamantane- <i>N</i> -oxyl for fast dye regeneration and open circuit voltages exceeding 1 V. Journal of Materials Chemistry A, 2019, 7, 10998-11006.	5.2	8
601	A Hierarchical 3D TiO <sub>2</sub> /Ni Nanostructure as an Efficient Holeâ€Extraction and Protection Layer for GaAs Photoanodes. ChemSusChem, 2020, 13, 6028-6036.	3.6	8
602	Illumination Time Dependent Learning in Dye Sensitized Solar Cells. ACS Applied Materials & Interfaces, 2018, 10, 36602-36607.	4.0	7
603	Bimetallic Electrocatalysts for Carbon Dioxide Reduction. Chimia, 2019, 73, 928.	0.3	7
604	A Novel Approach for the Detection of Geometric- and Weight-Related FSW Tool Wear Using Stripe Light Projection. Journal of Manufacturing and Materials Processing, 2020, 4, 60.	1.0	7
605	Nanosegregation in arene-perfluoroarene π-systems for hybrid layered Dion–Jacobson perovskites. Nanoscale, 2022, 14, 6771-6776.	2.8	7
606	Hyperbranched self-assembled photoanode for high efficiency dye-sensitized solar cells. RSC Advances, 2015, 5, 93180-93186.	1.7	6
607	A partially-planarised hole-transporting quart- <i>p</i> -phenylene for perovskite solar cells. Journal of Materials Chemistry C, 2019, 7, 4332-4335.	2.7	6
608	Effect of Corrosion and Surface Finishing on Fatigue Behavior of Friction Stir Welded EN AW-5754 Aluminum Alloy Using Various Tool Configurations. Materials, 2020, 13, 3121.	1.3	6
609	A Fully Printable Holeâ€Transporterâ€Free Semiâ€Transparent Perovskite Solar Cell. European Journal of Inorganic Chemistry, 2021, 2021, 3752-3760.	1.0	6
610	Carbazol-phenyl-phenothiazine-based sensitizers for dye-sensitized solar cells. Journal of Materials Chemistry A, 2021, 9, 26311-26322.	5.2	6
611	Determination of the Surface Concentration of Crown Ethers in Supported Lipid Membranes by Capacitance Measurements. Langmuir, 1998, 14, 2573-2576.	1.6	5
612	Nanocrystalline Injection Solar Cells. , 2006, , 363-385.		5

Nanocrystalline Injection Solar Cells. , 2006, , 363-385. 612

#	Article	IF	CITATIONS
613	Redox Catalysis for Improved Counterâ€Electrode Kinetics in Dyeâ€Sensitized Solar Cells. ChemElectroChem, 2017, 4, 1356-1361.	1.7	5
614	Photovoltaic Performance of Porphyrinâ€Based Dyeâ€5ensitized Solar Cells with Binary Ionic Liquid Electrolytes. Energy Technology, 2020, 8, 2000092.	1.8	5
615	Reduction of friction stir welding setup loadability, process forces and weld seam width by tool scaling. Proceedings of the Institution of Mechanical Engineers, Part L: Journal of Materials: Design and Applications, 2020, 234, 786-795.	0.7	5
616	Solid-state synthesis of CdFe2O4 binary catalyst for potential application in renewable hydrogen fuel generation. Scientific Reports, 2022, 12, 1632.	1.6	5
617	Thiocyanate-Mediated Dimensionality Transformation of Low-Dimensional Perovskites for Photovoltaics. Chemistry of Materials, 2022, 34, 6331-6338.	3.2	5
618	Effect of Interfacial Engineering in Solid‣tate Nanostructured Sb <sub>2</sub> S <sub>3</sub> Heterojunction Solar Cells (Adv. Energy Mater. 1/2013). Advanced Energy Materials, 2013, 3, 28-28.	10.2	4
619	Quasiâ€Solidâ€State Dyeâ€Sensitized Solar Cells Based on Ru(II) Polypyridine Sensitizers. Energy Technology, 2016, 4, 380-384.	1.8	4
620	Perovskite Films: Toward All Roomâ€Temperature, Solutionâ€Processed, Highâ€Performance Planar Perovskite Solar Cells: A New Scheme of Pyridineâ€Promoted Perovskite Formation (Adv. Mater. 13/2017). Advanced Materials, 2017, 29, .	11.1	4
621	Development of multijunction thin film solar cells. , 2009, , .		3
622	Substitution of Carbazole Modified Fluorenes as ï€-Extension in Ru(II) Complex-Influence on Performance of Dye-Sensitized Solar Cells. Advances in OptoElectronics, 2011, 2011, 1-10.	0.6	3
623	Introducing rigid π-conjugated peripheral substituents in phthalocyanines for DSSCs. Journal of Porphyrins and Phthalocyanines, 2016, 20, 1361-1367.	0.4	3
624	Fatigue Behavior of Conventional and Stationary Shoulder Friction Stir Welded EN AW-5754 Aluminum Alloy Using Load Increase Method. Metals, 2020, 10, 1510.	1.0	3
625	Characterization and Analysis of Effective Wear Mechanisms on FSW Tools. Minerals, Metals and Materials Series, 2021, , 21-34.	0.3	3
626	Effect of friction stir welding tool hardness on wear behaviour in friction stir welding of AA-6060 T66. Proceedings of the Institution of Mechanical Engineers, Part L: Journal of Materials: Design and Applications, 2022, 236, 1333-1345.	0.7	3
627	Tool Downscaling Effects on the Friction Stir Spot Welding Process and Properties of Current-Carrying Welded Aluminum–Copper Joints for E-Mobility Applications. Metals, 2021, 11, 1949.	1.0	3
628	Solar Cells: Ionic Liquid Control Crystal Growth to Enhance Planar Perovskite Solar Cells Efficiency (Adv. Energy Mater. 20/2016). Advanced Energy Materials, 2016, 6, .	10.2	2
629	Heteroleptic Ru(ii)-bipyridine complexes based on hexylthioether-, hexyloxy- and hexyl-substituted thienylenevinylenes and their application in dye-sensitized solar cells. Physical Chemistry Chemical Physics, 2016, 18, 11901-11908.	1.3	2
630	Why choosing the right partner is important: stabilization of ternary CsyGUAxFA(1â^'yâ^'x)PbI3 perovskites. Physical Chemistry Chemical Physics, 2020, 22, 20880-20890.	1.3	2

#	Article	IF	CITATIONS
631	Identifizierung von reaktiven Zentren und OberflÜhenfallen in Chalkopyritâ€Photokathoden. Angewandte Chemie, 2021, 133, 23843-23847.	1.6	2
632	Molecularly Engineered Low-Cost Organic Hole-Transporting Materials for Perovskite Solar Cells: The Substituent Effect on Non-fused Three-Dimensional Systems. ACS Applied Energy Materials, 2022, 5, 3156-3165.	2.5	2
633	Improved Stability of Solid State Light Emitting Electrochemical Cells Consisting of Ruthenium and Iridium Complexes. Materials Research Society Symposia Proceedings, 2006, 965, 1.	0.1	1
634	A Novel Efficient, Iodide-Free Redox Mediator for Dye-Sensitized Solar Cells. Materials Research Society Symposia Proceedings, 2007, 1013, 1.	0.1	1
635	Understanding the limit and potential in emerging perovskite solar cells. , 2017, , .		1
636	Understanding the Electrochemical Reduction of Carbon Dioxide at Copper Surfaces. ACS Symposium Series, 2019, , 209-223.	0.5	1
637	Influence of different Ni coatings on the long-term behavior of ultrasonic welded EN AW 1370 cable/EN CW 004A arrestor dissimilar joints. Welding in the World, Le Soudage Dans Le Monde, 2021, 65, 429-440.	1.3	1
638	Guanine‣tabilized Formamidinium Lead Iodide Perovskites. Angewandte Chemie, 2020, 132, 4721-4727.	1.6	0
639	Nanoscale interfacial engineering enables highly stable and efficient perovskite photovoltaics. , 0, , .		0
640	Advances in friction stir welding by separate control of shoulder and probe. Welding in the World, Le Soudage Dans Le Monde, 2021, 65, 1931-1941.	1.3	0
641	DYES AND MATERIALS FOR SENSITISED ELECTROCHEMICAL PHOTOVOLTAICS. , 2001, , .		0
642	Molelcular Photovoltaics and Perovskite Solar Cells. , 0, , .		0
643	Extraordinary Stability of Perovskite Solar Cells Yielding Photovoltage above 1.5V. , 0, , .		0
644	Watching Ions Move: Scanning Probe Microscopy on Perovskite Solar Cells. , 0, , .		0
645	Supramolecular Engineering of Layered Hybrid Perovskite Materials for Stable Perovskite Solar Cells. , 0, , .		0
646	Supramolecular Engineering of Layered Hybrid Perovskite Materials for Stable Perovskite Solar Cells. , 0, , .		0
647	Elucidation of Photovoltage Enhancements and Charge Transport in Multijunction Cu2O Photocathode through Semiconductor Simulations. , 0, , .		0
648	Watching Ions Move: Scanning Probe Microscopy on Perovskite Solar Cells. , 0, , .		0

Watching Ions Move: Scanning Probe Microscopy on Perovskite Solar Cells. , 0, , . 648

37

#	Article	IF	CITATIONS
649	Photoelectrochemical Oxygen Evolution on Mesoporous Hematite Films Prepared from Maghemite Nanoparticles. Journal of the Electrochemical Society, 2022, 169, 056522.	1.3	Ο
650	Holistic Passivation of Perovskite Solar Cells for Space Applications. , 0, , .		0
651	Reversible photo de-mixing in two-dimensional Dion-Jacobson mixed halide perovskites: photo-miscibility gap mapped. , 0, , .		0